frontiers | Frontiers in Nutrition

TYPE Original Research
PUBLISHED 08 February 2024
DOI 10.3389/fnut.2024.1351433

OPEN ACCESS

EDITED BY
Claude Billeaud,
Centre Hospitalier Universitaire de Bordeaux, France

REVIEWED BY
Oswaldo Hernandez-Hernandez,
Spanish National Research Council (CSIC), Spain
Jingyu Yan,
Chinese Academy of Sciences (CAS), China

*CORRESPONDENCE
Silvia Rudloff
✉ silvia.rudloff@ernaehrung.uni-giessen.de

RECEIVED 06 December 2023
ACCEPTED 18 January 2024
PUBLISHED 08 February 2024

CITATION
Kuntz S, Kunz C, Borsch C, Hill D, Morrin S, Buck R and Rudloff S (2024) Influence of microbially fermented 2′-fucosyllactose on neuronal-like cell activity in an *in vitro* co-culture system.
Front. Nutr. 11:1351433.
doi: 10.3389/fnut.2024.1351433

Influence of microbially fermented 2′-fucosyllactose on neuronal-like cell activity in an *in vitro* co-culture system

Sabine Kuntz[1], Clemens Kunz[1], Christian Borsch[1], David Hill[2], Sinéad Morrin[2], Rachael Buck[2] and Silvia Rudloff[1,3]*

[1]Department of Nutritional Science, Justus Liebig University Giessen, Giessen, Germany, [2]Abbott, Nutrition Division, Columbus, OH, United States, [3]Department of Pediatrics, Justus Liebig University Giessen, Giessen, Germany

Scope: 2′-Fucosyllactose (2′-FL), the most abundant oligosaccharide in human milk, plays an important role in numerous biological functions, including improved learning. It is not clear, however, whether 2′-FL or a cleavage product could influence neuronal cell activity. Thus, we investigated the effects of 2′-FL, its monosaccharide fucose (Fuc), and microbial fermented 2′-FL and Fuc on the parameters of neuronal cell activity in an intestinal–neuronal transwell co-culture system *in vitro*.

Methods: Native ^{13}C-labeled 2′-FL and ^{13}C-Fuc or their metabolites, fermented with *Bifidobacterium (B.) longum* ssp. *infantis* and *B. breve*, which were taken from the lag-, log- and stationary (stat-) growth phases of batch cultures, were applied to the apical compartment of the co-culture system with Caco-2 cells representing the intestinal layer and all-*trans*-retinoic acid-differentiated SH-SY5Y (SH-SY5Y$_{ATRA}$) cells mimicking neuronal-like cells. After 3 h of incubation, the culture medium in the basal compartment was monitored for ^{13}C enrichment by using elemental analysis isotope-ratio mass spectrometry (EA-IRMS) and effects on cell viability, plasma, and mitochondrial membrane potential. The neurotransmitter activation (BDNF, GABA, choline, and glutamate) of SH-SY5Y$_{ATRA}$ cells was also determined. Furthermore, these effects were also measured by the direct application of ^{13}C-2′-FL and ^{13}C-Fuc to SH-SY5Y$_{ATRA}$ cells.

Results: While no effects on neuronal-like cell activities were observed after intact 2′-FL or Fuc was incubated with SH-SY5Y$_{ATRA}$ cells, supernatants from the stat-growth phase of 2′-FL, fermented by *B. longum* ssp. *infantis* alone and together with *B. breve*, significantly induced BDNF release from SH-SY5Y$_{ATRA}$ cells. No such effects were found for 2′-FL, Fuc, or their fermentation products from *B. breve*. The BDNF release occurred from an enhanced vesicular release, which was confirmed by the use of the Ca^{2+}-channel blocker verapamil. Concomitant with this event, ^{13}C enrichment was also observed in the basal compartment when supernatants from the stat-growth phase of fermentation by *B. longum* ssp. *infantis* alone or together with *B. breve* were used.

Conclusion: The results obtained in this study suggest that microbial products of 2′-FL rather than the oligosaccharide itself may influence neuronal cell activities.

KEYWORDS

2′-fucosyllactose, fermentation, microorganisms, neuronal-like cell activity, BDNF

1 Introduction

Human milk oligosaccharides (HMOs) are the third largest solid component in human milk, present to the extent of 20–25 g/L in colostrum and 10–15 g/L in mature milk (1–5). 2′-Fucosyllactose (2′-FL) belongs to the fraction of fucosylated neutral HMOs and is quantitatively the most prominent component in the breastmilk of women expressing fucosyltransferase-2 (FUT-2), a phenotype referred to as secretor positive and representing 70–80% of the Western population (3–8). 2′-FL is a well-known structural homolog to bacterial adhesion sites in the intestine and may act as a prebiotic, supporting colonization of the colon with bacteria that may be beneficial to the breastfed infant (9–11).

In infants, breast milk feeding is known to provide significant health benefits and may even improve cognitive development and intellectual performance (12–16). In this context, 2′-FL or Fuc has been shown to affect cognitive domains and improve learning and memory in animal studies (17–19). 2′-FL is also associated with improved cognition (18, 20) and changes in brain tissue microstructure in breastfed infants (21). The mechanisms behind these neuronal effects are largely unknown. For example, a continuous administration of 2′-FL increased the expression of several molecules involved in the storage of newly acquired memories, such as the postsynaptic density protein 95, phosphorylated calcium/calmodulin-dependent kinase II, and brain-derived neurotrophic factor (BDNF) in cortical and subcortical structures (17). BDNF and its isoforms are members of the neurotrophin family and are synthesized by both, neuronal and non-neuronal cells. They are involved in processes such as differentiation and regeneration (22, 23). It has also been shown that BDNF plays a key role as a mediator of activity-induced long-term potentiation (LTP) in the hippocampus as well as in other brain regions (24). The role of BDNF and its isoforms in LTP is best studied in the hippocampus where the neurotrophins act at pre- and post-synaptic levels and are mediated by Trk (tropomyosin-related kinase) and the tumor necrosis factor receptor family, which are known to be coupled to the activation of the Ras/ERK, phosphatidylinositol-3-kinase/Akt and phospholipase C-g(PLC-g) pathways, and proBDNF/p75NTR/sortilin pathways (24–26). In addition, BDNF is the most important modulator of glutamatergic and GABAergic synapses and is also associated with glutamate and GABA through TrkB signaling (24, 27).

However, it is unclear whether 2′-FL itself or its metabolites are responsible for the observed effects. To achieve neuronal effects, 2′-FL or its metabolites may need to accumulate in the relevant brain regions; however, as we have recently shown, ^{13}C-labeled 2′-FL administered orally to wild-type and germ-free mice was unable to cross the healthy blood–brain barrier (28). A subsequent study showed that even the Fuc moiety from 2′-FL, administered as ^{13}C-labeled Fuc, was also not able to cross the blood–brain barrier either, although it was rapidly absorbed. It was observed that ^{13}C was enriched in the brain at time points after the oral bolus had reached the lower gut (29). This points to the influence of the intestinal microbiota, which are shown to metabolize HMOs and selectively promote the growth of beneficial microbiota such as bifidobacteria (30, 31). Metabolic studies in infants have demonstrated that 2′-FL in milk from secretor mothers is excreted via infants′ urine (32), which was confirmed by endogenously ^{13}C-labeled HMOs in breastfeeding mothers and the urinary excretion of ^{13}C-labeled HMO in their infants (33–36). Low amounts of 2′-FL have also been detected directly in the plasma of breastfed infants of secretor mothers compared to infants fed milk from non-secretor mothers or in plasma from formula-fed infants only when 2'FL was added as a supplement (37, 38). Despite the absorption of intact 2′-FL into the circulation, HMOs are not digested by human enzymes and reach the colon where they are metabolized by the infant gut microbiota.

In general, HMOs are substrates for beneficial microbes such as species of the *Bifidobacterium* genus, but it seems that only a few strains use HMOs as a preferred carbon source (39–43). However, the uptake of HMOs by microbial ABC transporters and their degradation by glycosyl hydrolases result in the formation of monosaccharides, which could be further metabolized by the fructose-6-phosphate phosphoketolase pathway into ATP, acetate, and lactate as end products, which was observed in the case of *B. longum* ssp. *infantis* (44–47). In contrast, extracellular glycosyl hydrolases of *B. breve* and *B. bifidum* generate metabolites that may serve as substrates for *B. longum* ssp. *infantis*, which highlights the co-existing or cross-feeding effects influencing HMO metabolism (48, 49). This microbe–HMO interaction was supported by an accumulation of HMO building blocks such as Fuc and trisaccharides after fermentation of HMO by bifidobacteria and lactobacilli, suggesting a symbiotic interaction of HMOs and specific gut microbiota (50). Recently, the analysis of the development of the gut microbiota of infants during the first month of life shows that colonization of FL-utilizing *Bifidobacteria* species is associated with altered metabolite profiles and microbiota composition (44). Equal co-cultures of bifidobacteria in 2′-FL-containing media produced different ratios of metabolites such as acetate and lactate under steady-state conditions when compared to monocultures (45). Furthermore, it has recently been confirmed that HMOs such as 2′-FL selectively promote the formation of a bifidobacteria-rich microbiota (30), which may then increase their potential impact on neurological functions via the gut–brain axis.

The overall aim of our *in vitro* intestinal–neuronal transwell co-culture system was to investigate if and how ^{13}C-labeled 2′-FL as well as its monosaccharide Fuc were metabolized by different *Bifidobacterium* species, alone or in combination, and if intact or subsequent metabolites cross the monolayers of Caco-2 cells cultured on transwell inserts to affect neuronal-like parameters in neuronal-like ATRA-differentiated SH-SY5Y$_{ATRA}$ cells.

2 Results

2.1 Effects of 2′-FL and Fuc on neurogenesis markers in neuronal-like cells before and after passage through an intestinal epithelial cell layer

To investigate the effects of 2′-FL and Fuc on neuronal-like cell activity markers, we used the human cell line SH-SY5Y, which had been differentiated by all-*trans*-retinoic acid (ATRA) into cells with a significant expression of the well-known neuronal marker synaptophysin (SYP) (51, 52) determined by flow cytometry (Figures 1A–C). Figure 1D shows that in the cultured SH-SY5Y

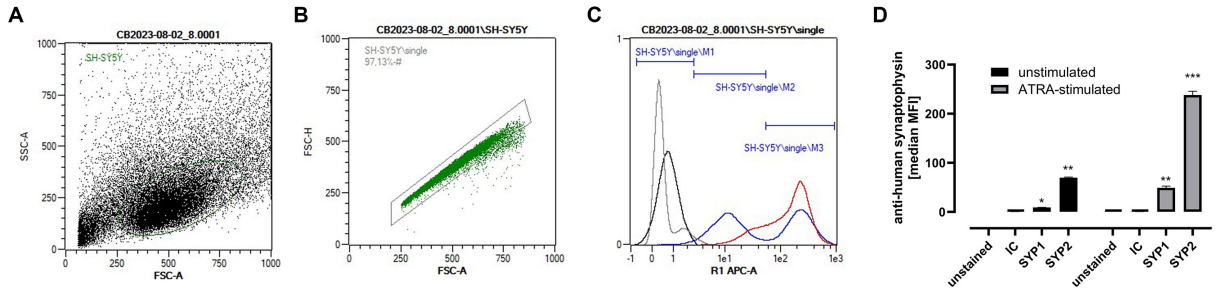

FIGURE 1
Synaptophysin (SYP) expression in SH-SY5Y and ATRA-differentiated SH-SY5Y cells. Differentiation of SH-SY5Y to SH-SY5Y$_{ATRA}$ was confirmed by measuring SYP expression by flow cytometry. Differentiated and non-differentiated cells were detached with accutase solution, centrifugated (500 × *g*, 5 min at RT) and stained according to the manufactures´ instructions (see Methods and Materials 4.1.2). The gating strategy for analyzing SYP expression is given for a representative staining in **(A–C)**. [**(A)** dotblot for cell gating (SSC-A vs. FSC-A), **(B)** dotblot for single cell inclusion (FSC-H vs. FSC-A), and **(C)** representative histogram of unstained cells (gray line), isotype control (IC) stained cells (black line), undifferentiated anti-human-SYP stained cells (blue line), and anti-human-SYP stained ATRA-induced cells (red line)]. **(D)** Quantification of the MFI (mean fluorescence intensity) was performed by setting histogram markers (M) for unstained and IC-stained cells (M1), low SYP (SYP1) expressing cells (M2), and high SYP (SYP2) expressing cells (M3). MFI data were performed using the MACSQuant 2.13.0 software and data analyses (medians with 95% CI) were performed with GraphPad Prism 10.0.2. Differences to IC-stained cells were significant at $*p < 0.05$, $**p < 0.01$, and $***p < 0.05$ (ANOVA with multicomparison test) for at least $n = 3$ (in duplicates).

cells, cell populations with both low and high SYP expression levels were present (Figure 1D). Incubation of these SH-SY5Y cells with ATRA over 10 days induced a significant enhancement of cells with high SYP expression, which is 2.6 times higher than in unstimulated cells.

These neuronal-like SH-SY5Y$_{ATRA}$ cells were used to investigate the effects of 2´-FL and Fuc with or without co-cultured Caco-2 cells (Figure 2A). Therefore, 2´-FL and Fuc were applied at non-cytotoxic concentrations (Figure 2B) to the apical side of the transwell (indirect incubation) or directly to SH-SY5Y$_{ATRA}$ cells. As shown in Figures 2C–F, incubation with ^{13}C-2´-FL and ^{13}C-Fuc (5 mM) at the apical side of the co-culture system did not result in any ^{13}C enrichment [δ^{13}C in $^{0}/_{00}$] in the basal compartments (Figure 2C, left *Y*-axis) compared to controls (5 mM glucose), nor did it induce BDNF release (Figure 2C, right *Y*-axis) in the supernatant or choline levels in the cells (Figure 2D). Consistent with these results, no changes in plasma membrane or mitochondrial potential were observed by direct or indirect incubation with 2´-FL or Fuc (Figures 2E,F).

These observations clearly indicate that neither 2´-FL nor Fuc had an influence on neuronal activity markers when they were applied to neuronal-like cells directly or indirectly. Due to the low concentration of intact 2´-FL or Fuc in systemic circulation and recently published data about the intense fermentation of 2´-FL and Fuc in the intestine of mice (28, 29), we aimed to investigate whether the fermentation of 2´-FL and/or Fuc by *Bifidobacterium* species had an influence on neuronal cell activity markers. Again, we used ^{13}C-labeled 2´-FL as well as Fuc. To gain further insight into the metabolic pathways of 2´-FL and/or Fuc during microbial fermentation, we used 2´-FL and Fuc either ^{13}C-labeled on C-atom 1 ($^{13}C_1$-Fuc) or 6 ($^{13}C_6$-Fuc).

2.2 Microbial fermentation of 2´-FL and Fuc

For fermentation studies, we used *B. longum* ssp. *infantis* and *B. breve* as bifidobacterial strains, as they are known to ferment HMOs by extra- and intracellular glycosyl hydrolases and have the potential for bifidobacterial cross-feeding (50). As shown in Figures 3A–C, all the bacterial strains grew well in media containing high concentrations of glucose (55 mM). *B. longum* ssp. *infantis*, *B. breve*, and co-cultured bifidobacteria grew rapidly and reached an optical density ($OD_{600\ nm}$) values of 1.58 ± 0.05, 1.39 ± 0.03, and 1.41 ± 0.05, respectively. When these strains were grown in media containing 5 mM glucose instead of 55 mM glucose, they still grew well, but with a lower maximum $OD_{600\ nm}$ values of 1.02 ± 0.07, 1.16 ± 0.05, and 1.25 ± 0.04 after 36 h of incubation, respectively (Figures 3A–C). Substitution of this lower glucose concentration of 5 mM with an isomolar concentration of 2´-FL as the sole carbohydrate source, *B. longum* ssp. *infantis* alone (Figure 3A) or in co-culture with *B. breve* (Figure 3C) grew to an optical density ($OD_{600\ nm}$) similar to that with 5 mM glucose (1.12 ± 0.07 and 1.16 ± 0.06). However, in media containing $^{13}C_1$-Fuc- or $^{13}C_6$-Fuc, *B. longum* ssp. *infantis* grew very slowly with maximum $OD_{600\ nm}$ values of 0.54 ± 0.02 and 0.52 ± 0.01. In contrast, *B. breve* showed better growth on $^{13}C_1$-Fuc and $^{13}C_6$-Fuc-containing media with a maximum optical density of 0.68 ± 0.01 and 0.63 ± 0.01, respectively, but did not grow in media containing ^{13}C-2´-FL as a carbohydrate source (Figure 3B).

To investigate the possible effects of fermentation products on neuronal cell activity makers, we collected growth media from 2´-FL- and Fuc-fermented batch cultures at three different time-points: lag-, log- and stat-growth phase. The collected supernatants were used in the intestinal–neuronal transwell co-culture system (Figure 4A).

2.3 Effects of bacterial fermentation products on SH-SY5Y$_{ATRA}$ cells in a co-culture model

In the first set of experiments, we aimed to investigate whether bacterial fermentation products collected at the three different time points during batch cultures passed an intestinal Caco-2 cell

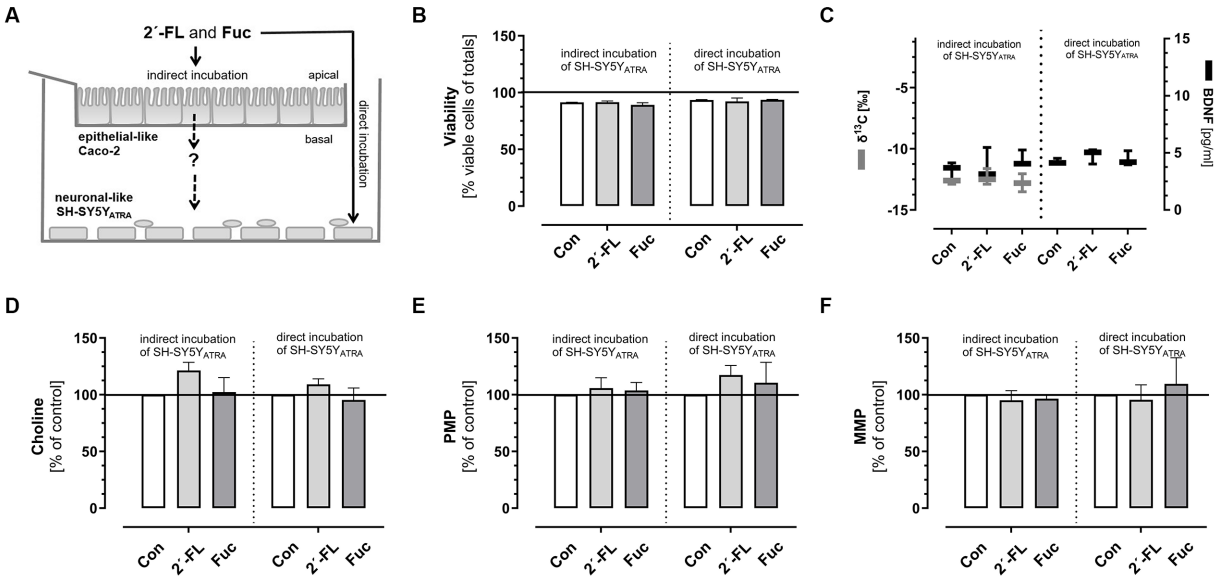

FIGURE 2
Determination of indirect and direct effects of 2´-FL and Fuc on ATRA-differentiated neuronal-like SH-SY5Y cells (SH-SY5Y$_{ATRA}$). Caco-2 cells, cultured on transwell inserts, were incubated with 2´-FL or Fuc (5 mM) for 3 h at 37°C. Thereafter, transwell inserts were removed and SH-SY5Y$_{ATRA}$ cells were further incubated with basal media (indirect incubation) or directly with 2´-FL or Fuc (0.5 mM) in comparison to controls (5 mM Glucose) **(A)**. Viability was measured by flow cytometry using the ViaCount Reagent® [% viable cells of total cells] **(B)**, ^{13}C enrichment [δ^{13}C in $^{0}/_{00}$] was determined by EA-IRMS [**(C)**, left *Y*-axis], BDNF concentrations [pg/mL] were measured in the supernatant by ELISA [**(C)**, right *Y*-axis], choline levels **(D)**, plasma membrane potential (PMP) and mitochondrial membrane potential (MMP) were determined fluorometrically and are given as % of controls **(E,F)**. Data are shown as box blots with min-max (whiskers) or as bars with means and standard deviation for $n = 3$ (each in duplicate). Significant differences were calculated by *t*-test comparing control with 2´-FL or Fuc.

monolayer and reached the basal compartment of the transwell system. In the second set of experiments, we measured BDNF secretion from SH-SY5Y$_{ATRA}$ cells after a 24 h incubation with the enriched basal media (Figures 4B–D).

Using cell-free media from different time points of bacterial growth, we observed significant ^{13}C enrichment and a concomitant BDNF secretion only with stat-growth phase 2´-FL metabolites from *B. longum* ssp. *infantis* in the basal compartments (Figure 4B) and, to a lesser extent, with 2´-FL metabolites from the stat-growth phase of *B. longum* ssp. *infantis* co-cultured with *B. breve* (Figure 4D). In the *B. breve* cultures, neither ^{13}C enrichment nor BDNF secretion by SH-SY5Y$_{ATRA}$ cells was observed with fermented 2´-FL metabolites (Figure 4C). However, when *B. breve* was incubated with ^{13}C-Fuc, ^{13}C enrichment was observed after the fermentation of Fuc (lag-growth phase) when C_6 atom of Fuc was ^{13}C-labeled, but not when $^{13}C_1$-Fuc was used. This was also observed when *B. breve* was *co*-cultured with *B. longum* ssp. *infantis*. Interestingly, no secretion of BDNF was observed by SH-SY5Y$_{ATRA}$ cells when Fuc metabolites were present in the basal media (Figures 4B–D).

In addition to BDNF, we could not detect any further effect on other potential neurotransmitters such as GABA (γ-aminobutyric acid) or the precursor molecule glutamate (see Supplementary Figures S1, S2). Further, it should be noted that the secretion of BDNF by differentiated neuronal-like cells was relatively low. Thus, the secreted amounts of BDNF in the co-culture system may not have been sufficient to influence further neurotransmitter release.

2.4 Effect of the calcium channel blocker verapamil on BDNF secretion from differentiated SH-SY5Y$_{ATRA}$ cells after incubation with bifidobacterial fermentation products

Based on the results with the stat-growth phase 2´-FL metabolites from *B. longum* ssp. *infantis* alone or grown together with *B. breve* on BDNF secretion by neuronal-like SH-SY5Y$_{ATRA}$ cells, we probed further with the aim of understanding the mechanism of the enhanced secretion. This secretion could be a result of increased mRNA expression or the release from secretory vesicles (53, 54). Therefore, we used Verapamil (VP) as a L-type calcium channel blocker to verify the effects on vesicular release and additionally RT-qPCR to measure mRNA expression. As shown in Figures 5A,B, BDNF release induced by 2´-FL metabolites from *B. longum* ssp. *infantis* was partially reduced by pre-incubation of SH-SY5Y$_{ATRA}$ cells with VP (Figure 5A). This effect was not observed for 2´-FL metabolites generated by *B. longum* ssp. *infantis* co-cultured with *B. breve* (Figure 5B). Due to the incomplete inhibition by VP, other calcium channels (e.g., N-, T-type) may also play a role. In contrast to the inhibiting effect of VP on BDNF release by *B. longum* ssp. *infantis*, we did not observe any changes in mRNA expression due to 2´-FL metabolites produced by *B. longum* ssp. *infantis* nor by *B. longum* ssp. *infantis* *co*-cultured with *B. breve* (see Supplementary Table T1).

Because of the well-known effect of neurotrophic factors on the Trk-signaling cascade (55), we measured the protein expression of the isoforms TrkA and TrkB on SH-SY5Y and SH-SY5Y$_{ATRA}$ cells. Both the isoforms were expressed on neuronal cells, but TrkB signaling is a

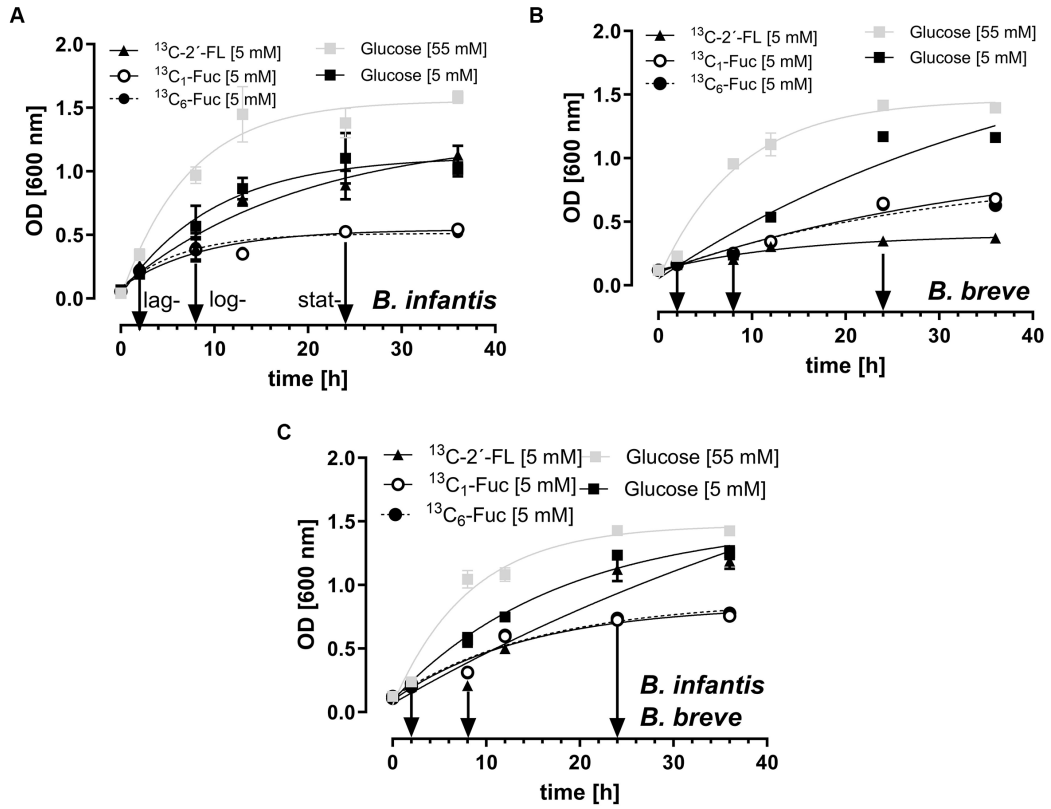

FIGURE 3
Growth of *B. longum* ssp. *infantis* **(A)**, *B. breve* **(B)**, and co-culture of *B. longum* ssp. *infantis with B. breve* **(C)** in high glucose-containing medium (55 mM), glucose-reduced media (5 mM), ^{13}C-2′-FL- and ^{13}C-Fuc-supplemented media (5 mM). Bacterial strains were anaerobically cultured at 37°C (see Methods and Materials 4.1.5) and growth was measured spectrophotometrically (600 nm). Data are given as means and standard deviation for $n = 3$. Arrows indicate the collection time of growth media at lag-, log- and stat-growth phase of the batch cultures.

well-known effect of BDNF, whereas TrkA signaling was induced by unprocessed BDNF (26, 56–58). Here (Figures 6A–H), we detected a slight but significant expression of TrkA (Figure 6F) and TrkB (Figure 6G) on unstimulated and ATRA-stimulated cells. Although BDNF has been found to increase the expression of TrkB as well as AChE (acetylcholine esterase) and ChAT activity (choline acyltransferase) (59, 60), we could not see any effect produced by the stat-phase supernatants of 2′-FL metabolized by *B. longum* ssp. *infantis* (Figure 6H).

3 Discussion

In the present study, we evaluated the effects of 2′-FL and Fuc, either as intact or fermented saccharides, on neuronal-like cell activity using an *in vitro* transwell co-culture model with intestinal Caco-2 cells, which reflect the intestinal cell layer in the gut, and ATRA-induced SH-SY5Y$_{ATRA}$ cells, which are used as a model of neuronal-like cells (61–63). These SH-SY5Y$_{ATRA}$ cells were either directly incubated with intact 2′-FL or Fuc or indirectly applied to a Caco-2 cell monolayer. In addition, 2′-FL and Fuc were fermented prior to the indirect incubation of SH-SY5Y$_{ATRA}$ cells to assess viability, neurotransmitter release, and changes in plasma membrane and also measure mitochondrial potential. While no effects on neuronal cell activities were detected on SH-SY5Y$_{ATRA}$ cells using intact 2′-FL or Fuc, metabolites from 2′-FL fermentation produced by *B. longum* ssp. *infantis* alone or together with *B. breve* showed an increase in BDNF secretion from SH-SY5Y$_{ATRA}$ cells in the *in vitro* co-culture model. Although only low levels of BDNF was secreted, it was a result of enhanced vesicular release and not a result of an induction of mRNA expression, as demonstrated by the use of the L-type calcium channel blocker Verapamil (VP).

HMOs are considered to exert effects in extra-intestinal tissues such as the brain (21, 64, 65). Many studies in this connection have reported that breastfeeding is associated with higher intelligence quotient (IQ), either at school age or in adulthood (20, 66, 67). Among the fucosylated oligosaccharides, *in vitro* administered 2′-FL and Fuc were able to enhance long-term potentiation (LTP) in the rat hippocampus (68, 69). In addition, Vázquez et al. (17) reported that synaptic plasticity in rodents was enhanced after oral supplementation with 2′-FL and Wu et al. (19) have recently shown that oral intake of 2′-FL improved locomotor activity and upregulated BDNF expression in rats. In another study, no significant differences were observed between 2′-FL-supplemented rats (age 4–6 weeks post weaning) and controls in behavioral tests such as the maze tests; however, significant differences were shown at age 1 year (20).

The underlying mechanisms are poorly understood and it has been speculated that a direct effect of 2′-FL in the brain or an indirect interaction with the vagus nerve at the intestinal level is possible (17, 70, 71). Despite the data showing that 2′-FL may reach the brain via

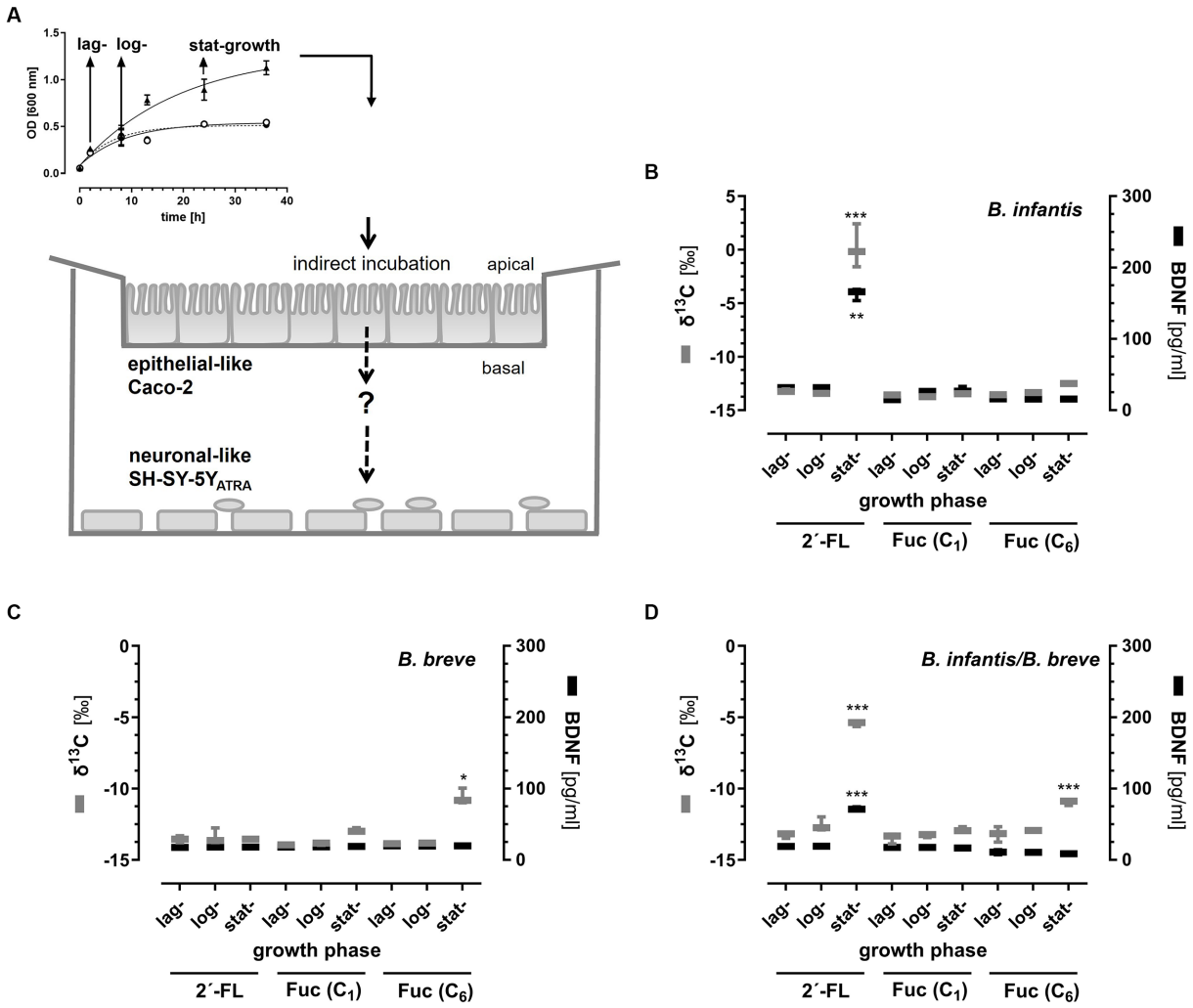

FIGURE 4
Enrichment of ^{13}C-2´-FL- and ^{13}C-Fuc-derived metabolites in the basal compartments of a transwell system and their influence on BDNF-secretion from neuronal-like SH-SY5Y$_{ATRA}$ cells. *B. longum* ssp. *infantis, B. breve*, and *B longum* ssp. *infantis* together with *B. breve* were grown in ^{13}C-2´-FL-, ^{13}C-Fuc (^{13}C$_1$-Fuc or ^{13}C$_6$-Fuc)-containing (5 mM) media. At the lag -, log-, and stat-growth phase, growth media were collected, centrifuged, filtered, and pH-adjusted (pH 7.4). Thereafter, supernatants were applied to the transwell inserts containing the Caco-2 cell monolayer (apical) and neuronal-like SH-SY5Y$_{ATRA}$ cells (basal) **(A)**. In the first set of experiments, basal compartments were collected after a 3 h incubation of Caco-2 cells to determine the ^{13}C enrichment by EA-IRMS being expressed as δ^{13}C [$^0/_{00}$] [**(B–D)** left *Y*-axis]. In a second set of experiments, SH-SY5Y$_{ATRA}$ cells were further incubated with basal media for 21 h to measure BDNF secretion by ELISA given as pg./mL [**(B–D)** right *Y*-axis]. Data are shown as box blots with min-max (whiskers) with n = 3 (each in duplicate). Significant differences between lag-, log-, and stat-growth phase values were calculated with one-way ANOVA with multi-comparison tests. Differences were significant at $*p < 0.05$, $**p < 0.01$, and $***p < 0.001$.

systemic circulation, we have recently shown that ^{13}C enrichment in the brain tissue does not occur when mice were given ^{13}C-labeled 2´-FL or Fuc via intravenous injection, indicating that none of these saccharides can cross the blood–brain barrier in mice. Furthermore, in germ-free mice orally fed with ^{13}C-labeled 2´-FL, the ^{13}C bolus remains in the intestinal content and was expelled via the feces, indicating that gut microbial metabolites of 2´-FL or Fuc could be responsible for the observed effects since ^{13}C enrichment of brain tissue occurred when the ^{13}C-2´-FL or ^{13}C-Fuc bolus had reached the lower gut containing microbiota (28, 29). In this context, it is well-known that bifidobacteria were able to utilize fucosylated HMOs to produce metabolites such as short-chain fatty acids (e.g., acetate) and lactate (72–74). During breastfeeding, *B. longum* ssp. *infantis* and *B. breve* are known to regularly colonize the infant gut and express several transport proteins and glycosidases directly involved in HMO utilization according to the HMO-degrading gene cluster. For example, *B. longum* ssp. *infantis* express transport proteins and intracellular 1,2-α-L-fucosidases or 1,3-1,4-α-L-fucosidases and therefore utilize HMO by transporting them from extracellular to intracellular sites and hydrolyzing them using glycoside hydrolases (74, 75).

In the present study, using our established intestinal–neuronal transwell co-culture system, we showed that intact ^{13}C$_1$-labeled 2´-FL or Fuc (^{13}C$_1$- and ^{13}C$_6$-labeled) were not able to cross the polarized Caco-2 cell layer as measured by EA-IRMS. Furthermore, using media in the basal compartment, we could not detect any effects on neuronal-like cell activities in SH-SY5Y$_{ATRA}$ cells when 2´-FL or Fuc was applied directly or indirectly via the Caco-2 layer. Based on these results,

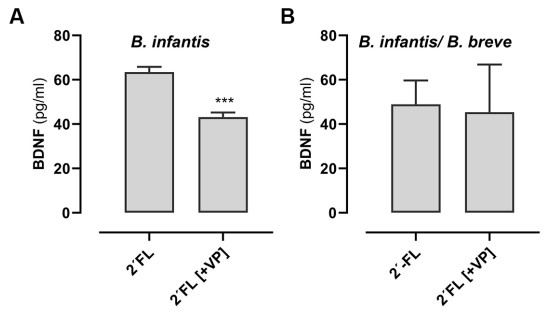

FIGURE 5
Effect of the calcium channel blocker verapamil (VP) on BDNF secretion from neuronal-like SH-SY5Y$_{ATRA}$ cells after incubation with stat-growth phase metabolite-enriched media. Neuronal-like SH-SY5Y$_{ATRA}$ cells were pre-incubated with 7.5 μM VP for 30 min or without VP. Thereafter, the cells were incubated for 24 h with the metabolite-enriched medium from stat-growth phase from *B. longum* ssp. *Infantis* **(A)** and *B. longum* ssp. Infantis co-cultured with *B. breve* **(B)**. After incubation with enriched media, BDNF secretion [pg/mL] was measured in the supernatant using ELISA (see Methods and Materials 4.4 and 4.9). Data are given as means ± standard deviation for $n = 3$ (in duplicates). Differences between cells with and without VP-treatment were analyzed with *t*-test and were significant at ***$p < 0.001$.

we used different *Bifidobacterium* strains to generate metabolites from 2′-FL or Fuc to further investigate their effects on neuronal-like cell activities. As expected, the bacterial strains *B. longum* ssp. *infantis* and *B. breve* alone or in combination showed different preferences with regard to 2′-FL and Fuc as carbohydrate growth substrates. *B. longum* ssp. *infantis* grew well on 2′-FL supplemented media very similar to an isomolar concentration of glucose, which was used as control. In contrast, *B. breve* preferred Fuc although to a much lower degree compared to the isomolar concentration of glucose; 2′-FL did not seem to be metabolized to support its growth. Co-incubation of *B. longum* ssp. *infantis* and *B. breve* revealed a more efficient fermentation of 2′-FL, when assessed by the pH levels (data not shown), achieved in the stationary phase of bacterial growth, suggesting an interaction of *B. longum* ssp. *infantis* and *B. breve* although a direct cross-feeding effect was not assessed.

To mimic the transport of bacterial metabolites from ^{13}C-labeled 2′-FL or Fuc across the intestinal epithelium, we collected supernatants at different time points (lag-, log- and stat-growth phase) of bacterial growth, applied them to a polarized Caco-2 cell monolayer, and measured ^{13}C enrichment in the basal compartment. While no ^{13}C enrichment was detected in lag- and log-growth phase supernatants, ^{13}C enrichment was observed in the stat-phase supernatants from *B. longum* ssp. *infantis* supplemented with 2′-FL and *B. breve* supplemented with Fuc, albeit in lower concentrations. Using supernatants from co-cultured *B. longum* ssp. *infantis* and *B. breve*, we also observed only an ^{13}C enrichment in the basal compartment with supernatants from the stat-growth phase. Interestingly, we detected the release of BDNF from SH-SY5Y$_{ATRA}$ cells only in stat-growth phase supernatants after 2′-FL fermentation from *B. longum* ssp. *infantis* containing batch cultures. Although we also observed a ^{13}C enrichment in stat-growth phase supernatants from $^{13}C_6$-Fuc-fermented bacterial strains, but not from $^{13}C_1$-Fuc, the ^{13}C enrichment was much lower than in the cultures with $^{13}C_1$-2′-FL. Nevertheless, it remains speculative whether the amount or type of metabolite was responsible for the BDNF releasing effect from SH-SY5Y$_{ATRA}$ cells. As mentioned above, *B. longum* ssp. *infantis* is able to degrade 2′-FL by several fucosidases, which may have released Fuc from 2′-FL. As the native Fuc applied directly to the differentiated cells did not produce any effect, it can be assumed that the effect was likely induced by metabolites. In this context, it has recently been shown that under anaerobic conditions Fuc was further metabolized to dihydroxyacetone-phosphate or lactate and/or 1,2-propanediole (1,2-PDO), which are intermediate productions for the generation of short chain fatty acids, i.e., lactate is a precursor of acetate and butyrate and 1,2-PDO of propionate (76). Keeping in mind that C_1 of Fuc was ^{13}C-labeled, ^{13}C enrichment may rather be derived from a dihydroxyacetone phosphate metabolite than from a lactate and/or 1,2-PDO metabolite, since lactate and/or 1,2-PDO are C4,5,6-backbone molecules, whereas dihydroxyacetone phosphate results from the C1,2,3-backbone (76–78). On the other hand, it has been shown that metabolites such as lactate play an important role in LTP. A pharmacological inhibition of MCT2 (monocarboxylate transporter 2), a transporter delivering lactate to neurons, irreversibly impairs long-term memory possibly by modulating the PGC1α/FNDC5/BDNF pathway (79–81). We expected that the use of Fuc labeled either on C_1 or C_6 of the molecule should enable us to gain further insight into the metabolic pathways of Fuc. However, we showed that 2′-FL labeled on C_1 of its Fuc moiety had been metabolized by *B. longum* ssp. *infantis*, but not ^{13}C-labeled compounds, which were able to pass an intestinal cell layer when ^{13}C-labeled Fuc was infused, labeled on either C_1 or C_6 of the molecule. In addition, we observed that Fuc degradation by *B. breve* led to soluble compounds containing the C_6-atom from Fuc; the C_1-ending of Fuc might have been completely metabolized, e.g., to CO_2 since no ^{13}C enrichment was seen in the basal compartment when $^{13}C_1$-Fuc was supplemented to bacterial media. Which metabolite is responsible for the ^{13}C enrichment in the basal compartment after incubation of Caco-2 cells with media from *B. longum* ssp. *infantis* or the mixture of *B. longum* ssp. *infantis* and *B. breve* needs further investigation. However, only metabolites from 2′-FL produced from *B. longum* ssp. *infantis* were able to induce secretion of BDNF in SH-SY5Y$_{ATRA}$ cells.

As mentioned above, BDNF and its isomers are members of the neurotrophin family and have been shown to play a key role as mediators of activity-induced LTP in neuronal cells. It has been shown that BDNF mRNA expression could be induced in SH-SY5Y cells by different stimuli (54, 82) and the released BDNF protein could act at auto- and paracrine levels. As such, it is an important modulator of glutamatergic and GABAergic synapses with glutamate and GABA release through TrkB receptor signaling (27). In this context, the released BDNF binds to TrkB and activates Ras/ERK, phosphatidylinositol3-kinase/Akt and phospholipase C-g(PLC-g) signaling cascades, which in turn stimulate glutamate and GABA release as neurotransmitters (24, 25, 80). BDNF release, however, is a highly regulated process in which ER (endoplasmic reticulum)- and Golgi-associated vesicles are released either constitutively or through regulated mechanisms. The secretion via Golgi-derived vesicles requires Ca^{2+}-sustained intracellular elevations and is associated with plasma membrane hyperpolarization. In addition, TrkB activation by BDNF triggers the PGC1α (peroxisome proliferator-activated receptor- γ coactivator 1-alpha) pathway, which in turn increases the expression of BDNF protein (80, 83). In our experiments, metabolites from 2′-FL produced by

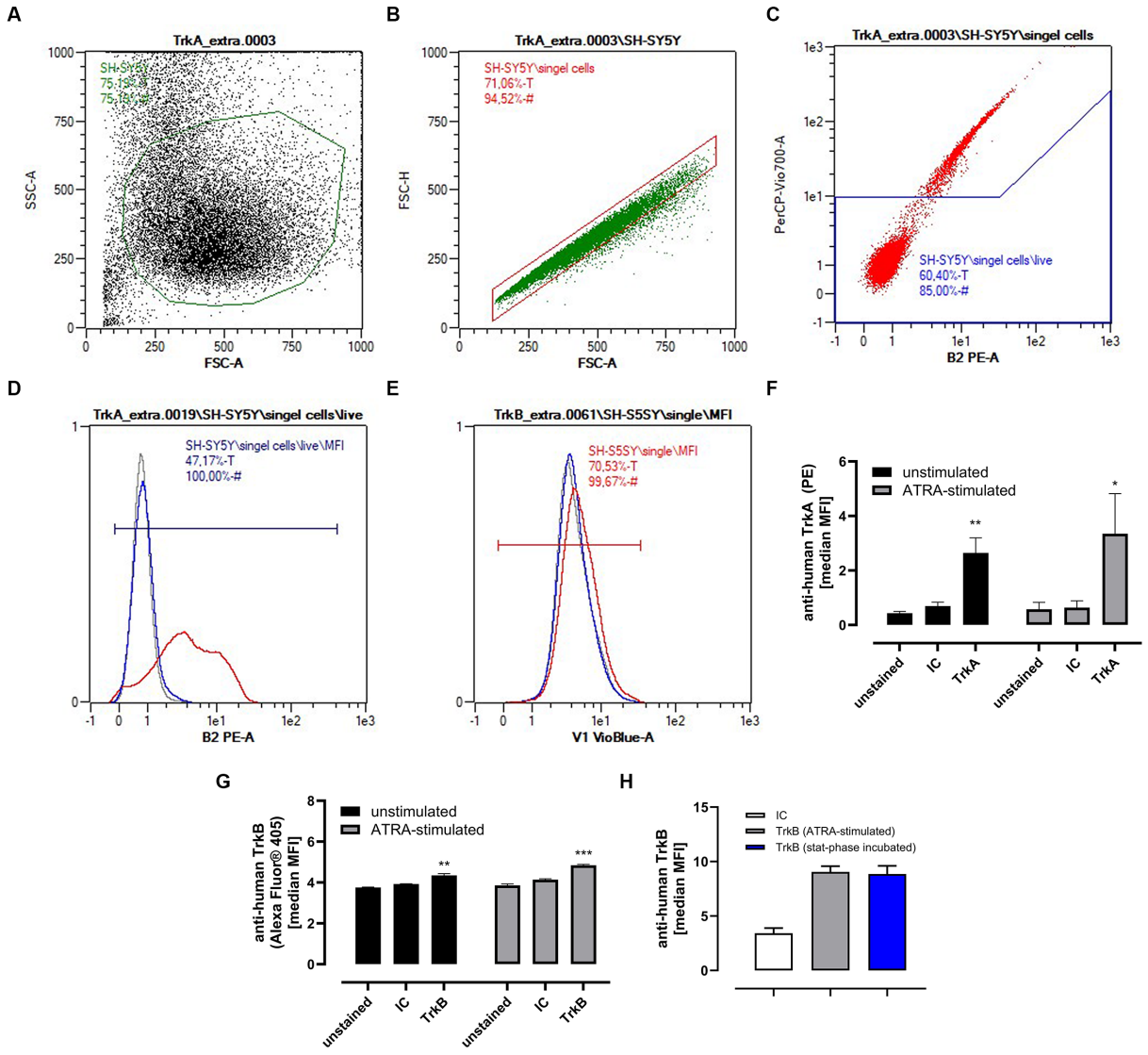

FIGURE 6
Expression of TrkA and TrkB in unstimulated SH-SY5Y and ATRA-stimulated SH-SY5Y$_{ATRA}$ cells and the effect of metabolites from stat-growth phase supernatant from 2´-FL fermentation by *B. longum* ssp. *infantis*. Cells were incubated with or without ATRA (see Section 4.1.2) and expression of TrkA and TrkB was analyzed by flow cytometry (see Section 4.10). Therefore, after incubation, cells were treated with accutase solution to ensure surface protein integrity. After centrifugation (500 × *g*, 5 min), harvested cells (1 × 10^5 cells/mL) were incubated with anti-human TrkA PE-conjugated, anti-human TrkB Alexa Fluor® 405-conjugated monoclonal antibody or with corresponding isotype control (IC) for 10 min in the dark at room temperature. Gating strategy for analyzing TrkA and TrkB with MQ10 Analyzer for a representative staining is given in **(A–C)**. [single cells (FSC-H vs. FSC-A) **(B)**, propidium iodide-stained cells (PerCP-Vio700A vs. PE) **(C)**, representative histogram overlay of unstained (gray), isotype stained (blue line) and ATRA-stimulated Trk stained cells (red line) **(D, E)**]. Quantification of TrkA **(F)** and TrkB, **(G)** expression and influence of 2´-FL metabolite enriched media on TrkB expression **(H)**. Data are given as MFI (main fluorescence intensity) medians with CI (95%) for $n = 3$ (each in duplicates) and quantification was performed using the MACSQuant 2.13.0 software. Data analysis were performed with GraphPad Prism 10.0.2. Significant differences between IC were calculated with One-way ANOVA with multi-comparison tests. Differences were significant at $^*p < 0.05$, $^{**}p < 0.01$, and $^{***}p < 0.001$.

Bifidobacterium species did not affect the BDNF gene expression as confirmed by RT-qPCR but did induce a low, but significant BDNF release. Using Verapamil, a well-known L-type voltage-dependent calcium channel (VDCC) antagonist that inhibits BDNF release (84), we observed a significant, but not complete inhibition of BDNF secretion, suggesting that additional mechanisms are involved in the release of BDNF from SH-SY5Y$_{ATRA}$ cells. This was also reported for primary neuronal cells using Verapamil as a VDCC blocker (85). Other than the observed secretion of BDNF, no further influence on choline, glutamate, or GABA release was detected, possibly due to the low levels of secreted BDNF and an unexpectedly low TrkB expression on SH-SY5Y$_{ATRA}$ cells. Thus both the low BDNF secretion and the lack of signaling activation described above could be offered as an explanation, although TrkB receptor expression has previously been shown to be present in SH-SY5Y cells after differentiation with retinoic acid (86). In this context, it should be mentioned that several differentiation protocols for the neuroblastoma cell line SH-SY5Y into a neuronal-like cell type have been established using

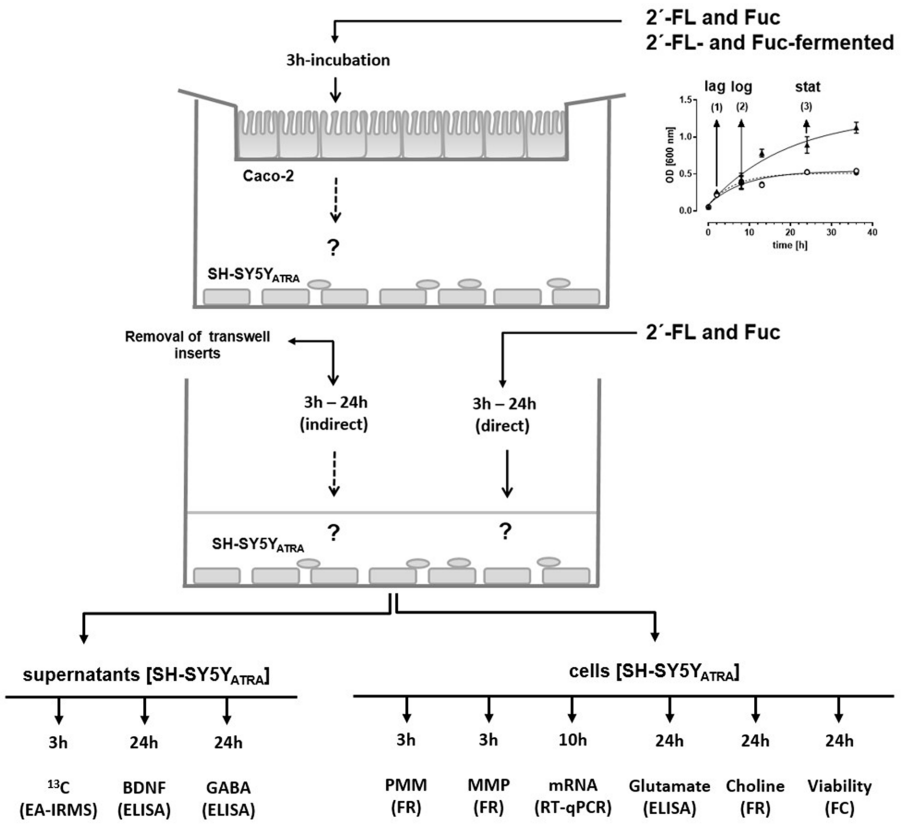

FIGURE 7
In vitro transwell intestinal-neuronal co-culture model. Non-fermented ^{13}C-2´-FL (5 mM) and ^{13}C-Fuc (5 mM) as well as ^{13}C-2´-FL or ^{13}C-Fuc fermented by *B. longum* ssp. *infantis, B. breve,* and *B. longum* ssp. *infantis /B. breve,* collected at the lag-, log-, and stat-growth phase, were applied to the transwell inserts cultivated with 22-day differentiated Caco-2 cells ("indirect incubation"). After a 3 h of incubation, Caco-2 inserts were removed and 10-day ATRA-differentiated SH-SY5Y cells (SH-SY5Y$_{ATRA}$) were used immediately or incubated for the times indicated to measure neuronal cell activities. For "direct" incubation, ^{13}C-2´-FL (0.5 mM) and ^{13}C-Fuc (0.5 mM) were incubated with SH-SY5Y$_{ATRA}$ cells. After indicated incubation times of SH-SY5Y$_{ATRA}$ cells, basal compartments (supernatants) were collected to measure ^{13}C enrichment by EA-IRMS, BDNF, and GABA concentrations by ELISA. Cells were used to measure membrane potential [plasma (PMM) and mitochondrial (MMP)] and choline levels by fluorescence kits using a fluorescence reader (FR), mRNA-expression of BDNF by real-time quantitative PCR (RT-qPCR), glutamate by ELISA, and viability by flow cytometry (FC).

ATRA, B27-supplement, and BDNF, alone or in combination (59, 62, 87).

In conclusion, our ATRA/B27-supplement treatment of SH-SY5Y cells revealed a neuronal-like phenotype with increased expression levels of synaptophysin, a well-known marker of neuronal cell differentiation. Using this neuronal-like cell model, we have shown that only 2´-FL, fermented by *B. longum* ssp. *infantis* induced BDNF secretion via vesicle-releasing mechanisms. However, it remains to be determined which metabolite may be responsible for ^{13}C enrichment and the effect of neuronal cell activity.

4 Methods and materials

4.1 Study design

In order to investigate the effects of non-fermented and fermented 2´-FL and Fuc on neuronal cell activity markers, we developed an *in vitro* transwell co-culture model in which human intestinal epithelial cells (Caco-2) and ATRA-differentiated SH-SY5Y neuronal-like cells (SH-SY5Y$_{ATRA}$) were able to impact each other (Figure 7) similar to our previously published *in vitro* epithelial-endothelial co-culture model (88). In order to mimic the absorption and metabolization sites in the intestine, Caco-2 cells were grown on semipermeable transwell filters over 22 days to differentiate and develop an enterocyte-like phenotype. After differentiation, transwell filters were inserted into a 24-well cavity where SH-SY5Y$_{ATRA}$ cells were cultivated at the bottom of the cavity. The upper compartment (transwell insert) with epithelial cells was exposed with non-fermented and fermented 2´-FL and Fuc for 3 h (indirect incubation). Thereafter, inserts were removed and basal media (supernatants) as well as SH-SY5Y$_{ATRA}$ cells were used immediately or after indicated times in order to determine neuronal cell activity markers. Direct incubation was done using intact 2´-FL and Fuc directly on SH-SY5Y$_{ATRA}$ cells.

4.1.1 Culturing intestinal Caco-2 cells

The human intestinal epithelial cell line Caco-2 (HTB37™) was derived from colon adenocarcinoma cells obtained from ATCC (Manassas, Virginia, United States). The cells were routinely grown in 75 cm^2 culture flasks using Dulbecco's Eagle's Minimum Essential Medium (DMEM) at pH 7.4 with 1% non-essential amino acids (NEAA), 1% sodium pyruvate, and 10% fetal calf serum (FCS,

TABLE 1 Antibodies for Synaptophysin staining of SH-SY5Y and SH-SY5Y$_{ATRA}$ cells.

Target	Primary recombinant antibodies (Ab)	Fluorochrome	Dilution	Incubation time	MQ10 channel
Synaptophysin (SYP), clone REA1121	REAfinity®	APC	1:50	10 min	R1 (APC)
Isotype control for SYP	Recombinant human IgG1	APC	1:50	10 min	R1 (APC)

Invitrogen, Germany). Cells were maintained in a humidified atmosphere of 5% CO_2 in air at 37°C. Stock passages were sub-cultured every 4 days until reaching 70–80% confluence. For incubation studies, pre-confluent cells were trypsinized with a 0.25% (w/v) trypsin/0.53 mM EDTA solution (Invitrogen, Darmstadt, Germany) and 1×10^4 cells per 0.5 mL^{-1} were seeded onto a 24-well transwell-insert with a polycarbonate membrane (0.4 µm pore size, Greiner-Bio-One GmbH, Frickenhausen, Germany) and placed in a 24-well cavity. Cells were allowed to grow to confluence (2 days) with DMEM (20% FCS) and thereafter to differentiate to absorptive enterocytes within 22 days. The culture medium was changed every 2–3 days at the apical (0.5 mL) and basolateral sides (1.5 mL). For incubation experiments at day 22, the transepithelial electrical resistance (TEER), a marker of the integrity of polarized epithelial cell monolayers, was determined before and after the experiments by using a Millicell® ERS volt-ohmmeter (Millipore Corporation, Bedford, MA, United States). TEER readings were taken at 37°C after equilibrium with the incubation media. A TEER value ≥800 Ohm × cm^2 was used as an indicator for an intact epithelial layer suitable to be used for incubation studies.

4.1.2 Culturing neuroblastoma SH-SY5Y cells

The human neuroblastoma cell line SH-SY5Y (ACC209) was obtained from DSMZ (German Collection of Microorganisms and Cell Cultures GmbH, Braunschweig, Germany). Cells were cultured (5% CO_2; 37°C) in Ham's F12/DMEM (1:1; with GlutaMAX™, sodium bicarbonate and sodium pyruvate) and supplemented with 15% FCS (Invitrogen GmbH, Karlsruhe, Germany). Cells were routinely sub-cultured splitting sub-confluent cultures (70–80%) 1:10 with 0.5% (w/v) trypsin/0.25 mM EDTA solution (Invitrogen GmbH, Karlsruhe, Germany). Cells grow as undifferentiated, continuously proliferating cells and include both adherent and floating cells. For sub-cultivation, one third of the supernatant with floating cells was collected, centrifugated (500 × *g*, 5 min at RT) and taken up in fresh complete media. Pre-confluent adherent cells were trypsinized with a 0.5% (w/v) Trypsin/0.25 mM EDTA solution and after centrifugation (500 × *g*, 10 min at room temperature), 1×10^5 cells ml^{-1} were seeded into a new culture flask and combined with the pre-collected floating cells. For incubation studies (direct or indirect (co-culture system)), adherent and floating SH-SY5Y cells were cultured in serum-reduced medium (2.5% FCS) containing 10 µM all-*trans*-retinoid-acid (ATRA) (Merck, Darmstadt, Germany) on a 24-well-plate and allowed to differentiate within 8 days according to Teppola et al. (89) and Al-Maswary et al. (90) with slight modification. After 24 h of sub-culturing, serum reduced medium was replaced with a medium containing B-27™ supplement (ThermoFischer Scientific, Darmstadt, Germany) and 10 µM ATRA to promote differentiation into a neuronal-like phenotype. Stock solution of ATRA was diluted in 96% ethanol and the final ethanol concentration did not exceed 0.1% in cell culture medium. Control cells were treated with vehicle (0.1% ethanol). This treatment was replaced every 3 days to replenish ATRA in culture media and, after the differentiation protocol, SH-SY5Y$_{ATRA}$ differentiation was confirmed by flow cytometry with SYP as a well-known neuronal marker (51, 52). Therefore, after detachment of SH-SY5Y$_{ATRA}$ cells with accutase solution (PromoCell GmbH, Heidelberg Germany), cells were centrifugated (500 × *g*, 5 min at RT) and stained according the manufacturer's instructions with slight modifications. Centrifuged cells were resuspended in 100 µL MACS buffer (Miltenyi Biotec B.V. & Co. KG, Bergisch-Gladbach, Germany) and were fixed for 20 min in darkness with 150 µL Cyto Fast Perm FIX buffer (BioLegend®, Amsterdam, Netherland). After washing, step cells were permeabilized and stained with 98 µL Cyto Fast Perm solution with 2 µL anti-human Synaptophysin-APC REAfinity antibody (Miltenyi Biotec B.V. & Co. KG) for 10 min at room temperature (Table 1). Unbound antibodies were removed by washing the cells in 1 mL running buffer (Miltenyi Biotec B.V. & Co. KG). After centrifugation (500 × *g*, 10 min), cells were resuspended in 200 µL of MACS running buffer for final flow cytometry analysis in R1-APC channel. Cell gating strategy and quantification (Figures 1A–D) were performed using the MACSQuant 2.13.0 software (Miltenyi Biotec B.V. & Co. KG) by comparing the median fluorescence intensities (MFI) of unstained, isotype stained and SYP-stained cells with at least $n = 3$ (each done in duplicates).

4.1.3 Co-culturing intestinal and neuronal-like cells with a transwell system

In order to investigate the effects of non-fermented and fermented 2′-FL and Fuc on neuronal-like cells, we developed an *in vitro* transwell co-culture system with human intestinal epithelial cells (Caco-2) and SH-SY5Y$_{ATRA}$ cells (Figure 7). According to the experimental setting, differentiated Caco-2 cells on transwell filter inserts were placed onto a 24-well plate, where SH-SY5Y$_{ATRA}$ cells had been cultured as described above. In a first set of experiments, non-fermented 2′-FL and Fuc were exposed directly to SH-SY5Y$_{ATRA}$ cells in order to evaluate the direct effect on neural activity markers. In a second set of experiments, non-fermented and fermented 2′-FL and Fuc were exposed to the upper compartment with Caco-2 cells on transwell filters (indirect incubation) (see Section 4.1).

4.1.4 Isotope-labeled 2′-FL and Fuc

Stable isotope labeled 2′-FL containing the C-atom 1 in the fucose ring as ^{13}C ([1 -^{13}C$_1$]-2′-FL (^{13}C-2'FL)) was obtained from ELICITYL (Crolles, France). In addition, we used L-Fuc, which was ^{13}C-labeled either at C$_1$ [^{13}C$_1$-Fuc] or C$_6$ [^{13}C$_6$-Fuc] also with a ^{13}C enrichment of 99% (ELICITYL). Both were used either at a concentration of 0.5 mM for direct incubation or 5 mM for the fermentation studies (indirect incubation).

4.1.5 Bacterial fermentation of 2´-FL and Fuc

2´-FL or Fuc metabolites were generated by batch cultivation of 2´-FL or Fuc with *B. longum* ssp. *infantis* (DSM 20088) obtained from the German Collection of Microorganisms and Cell Cultures GmbH (DSMZ, Braunschweig, Germany) and with *B. breve* (DSM 20213) as a gift from Prof. Dr. Sylvia Schnell (Department of Applied Microbiology, Justus-Liebig University Giessen, Germany). Rehydration of freeze-dried bacterial strains and −80°C stock cultures were done according to the manufacturer's instructions. *B. longum* ssp. *infantis* and *B. breve* were routinely cultured at 37°C in 'Bifidobacterium medium' containing 10 g/L casein peptone (tryptic digest), 10 g/L glucose, 5 g/L yeast extract, 5 g/L meat extract, 5 g/L bacto soytone, 2 g/L K_2HPO_4, 0.2 g/L $MgSO_4{\cdot}7H_2O$, 0.05 g/L $MnSO_4{\cdot}H_2O$, 1 mL/L Tween80, 5 g/L NaCl, 40 mL salt solution (0.25 g/L $CaCl_2{\cdot}2\ H_2O$, 0.5 g/L $MgSO_4{\cdot}7H_2O$, 1.0 g/L K_2HPO_4, 1.0 g/L KH_2PO_4, 10.0 g/L $NaHCO_3$, 2.0 g/L NaCl), and 4 mL/L resazurin (250 mg/L) dissolved in distilled water and autoclaved at 121°C for 40 min. Thereafter, the medium was left within the autoclave until reaching 98°C and was then further cooled down under oxygen-free gas (10% CO_2, 80% N_2, and 10% H_2) to avoid redissolving of oxygen. After autoclavation, pH was adjusted to pH 6.8 using NaOH (8 M) and supplemented with sterile filtered 0.5 g/L L-cysteine hydrochloride. Then, the medium was dispensed into Hungate anaerobic culture tubes under gas. Both strains were grown in independent triplicates under anaerobic condition at 37°C and growth was assayed by the determination of an increase in optical density (OD) at 600 nm using Shimadzu UV 1001 spectrophotometer (Shimadzu GmbH, Duisburg, Germany).

For incubation studies, corresponding bacterial growth media was prepared glucose-free and substrate utilization was determined by adding sterilized glucose or ^{13}C-labeled compounds to glucose-free medium. To obtain working cultures, cultivated stock cultures were incubated three times in carbohydrate-reduced medium to adapt microorganisms to the incubation media. After inoculation with bacterial suspensions for *in vitro* co-culture experiments, samples were taken at three different time points: the lag-growth phase, the logarithmic growth phase (log-growth phase), and stationary growth phase (stat-growth phase). After centrifugation (5 min, 13,000 rpm), the bacteria-free culture media were filtered through a 0.2 µm PES Whatman syringe filters (FisherScientific, Schwerte, Germany) and were used immediately for functional assays or stored at −80°C until for further analyses.

4.2 Determination of ^{13}C enrichment by elemental analysis isotope mass spectrometer

To analyze cell culture samples for ^{13}C enrichment, 0.15 mg liquid samples (apical cell culture samples) were weighted into tin capsules containing 5 mg of acid-washed Chromosorb W (IVA Analysentechnik e.K., Meerbusch, Germany). Triplicate samples were subjected to Elemental Analysis Isotope Ratio Mass Spectrometry (EA-IRMS) as described previously (28). Measurements and calculations were performed using the IonVantage Software v1.7 in combination with Ionos v4.2; both software applications were obtained from Elementar UK (Stockport, United Kingdom). Results are expressed as δ^{13}C enrichment [‰] with VPDB being the international standard obtained from the International Atomic Energy Agency (IAEA, Vienna, Austria).

4.3 Viability

A subset of cultured SH-SY5Y$_{ATRA}$ cells was used for measuring cell viability to ensure the viability of cells during co-cultivation by using the ViaCount™-assay (Luminex BV, MV ´s-Hertogenbosch, Netherland). Thus, cells were trypsinized using a 0.5% (w/v) trypsin/0.25 mM EDTA solution (Invitrogen) after 24 h incubation. After centrifugation (500 × *g*, 10 min), the pelleted cells were suspended in 500 µL of PBS. Following this, 20 µL of the cell solution was incubated with 480 µL ViaCount-Reagent™ and incubated for 10 min in the dark at 37°C. Immediately after Live/Dead-staining, cells were measured by flow cytometry on the Guava EasyCyte Mini Flow Cytometer (Guava Technologies, Merck Millipore, Darmstadt, Germany). Viability was expressed as % viable cells of totals with the Guava® software ($n = 3$, each done in duplicates). Further, 480 µL of the cell solution were used for glutamate detection in cell lysates (see Section 4.4).

4.4 Detection of neurotransmitters (BDNF, GABA, and glutamate)

The secretion of the neurotransmitter BDNF and GABA were measured in the supernatant of 24 h- stimulated SH-SY5Y$_{ATRA}$ cells using BDNF Quantikine™ ELISA Kit (R&D, Heidelberg, Germany) and ELISA kit for GABA (Abcam, Rozenburg, Germany). Glutamate as a precursor for GABA was measured in SH-SY5Y$_{ATRA}$ cell lysates according to the manufacturer's instructions with the Glutamate ELISA Kit (Abcam). Briefly, after incubation of the SH-SY5Y$_{ATRA}$, supernatants were collected and stored at –20°C until analysis for BDNF and GABA. For glutamate quantification, 480 µL of trypsinized SH-SY5Y$_{ATRA}$ cells (see Section 4.3) was used immediately and washed twice with PBS and lysed with lysis buffer for 20 min. Afterward, lysed cells were centrifugated (500 × *g*, 10 min) and supernatant was collected and used according to the manufacturer's instructions (Abcam). BDNF and GABA concentrations were measured at 450 nm and glutamate concentration were measured at 405 nm using the DigiScan microplate reader (Asys, Eugendorf, Austria). The BDNF and GABA concentrations were expressed as pg./mL and glutamate concentrations were expressed as µg/mL with $n = 3$ (each done in duplicates).

4.5 Choline levels

The total choline levels (free choline and acetylcholine) in SH-SY5Y$_{ATRA}$ cells were measured using the fluorometric Choline/Acetylcholine Assay Kit (Abcam) in freshly prepared samples according to the manufacturer's instructions. Briefly, after direct or indirect incubation of SH-SY5Y$_{ATRA}$ cells, cells were harvested by trypsinization (0.5% (w/v) trypsin/0.25 mM EDTA solution) and were washed twice with ice-cold PBS (Invitrogen GmbH). The cell pellet was resuspended in 500 µL choline assay buffer and homogenized by pipetting up and down ten times and leaving the cells for 10 min on

ice. After centrifugation (500 × *g*, 5 min, 4°C), the supernatant was collected and the assay was done according to the manufacturer's instructions. Acetylcholine was converted to choline by adding acetylcholinesterase and free choline was oxidized via the intermediate betaine aldehyde to betaine. The reaction generates products, which react with the choline probe to generate a fluorescence signal (Ex/Em 535/585 nm). Total choline concentrations were measured in black-clear microtiter plates (Greiner Bio-One GmbH, Frickenhausen, Germany) using the Ascent microplate fluorescence reader (Thermo Fisher Scientific, Germany). Fluorescence values (RFU) were finally expressed as % of controls with $n = 3$ (each done in duplicates).

4.6 Plasma membrane potential

Plasma membrane potential (PMP) was measured with the fluorogenic membrane Assay Kit (Abcam) according to the manufacturer's instructions. Briefly, after "direct" incubation of SH-SY5Y$_{ATRA}$ cells with 2′-FL and Fuc for 3 h or "indirect" incubation with basal media from transwell studies, the medium was replaced with 150 µL assay buffer (1:10) including 2 µL MP sensor dye. After 30 min of incubation in a 5% CO_2 incubator, fluorescence intensity (Ex/Em 535/585 nm) was measured using the Ascent microplate fluorescence reader (Thermo Fisher Scientific). Fluorescence values (RFU) were finally expressed as % of controls with $n = 3$ (each done in duplicates).

4.7 Mitochondrial membrane potential

Mitochondrial membrane potential (MMP) was measured with the fluorogenic JC-1 Assay Kit (Abcam) according to Sakamuru et al. (91). Briefly, after `direct´ incubation of ATRA-differentiated SH-SY5Y cells with 2′-FL and Fuc over 3 h or `indirect´ incubation with basal media from transwell studies, the medium was replaced with 200 µL HBSS buffer including 5 µM JC-1 solution (5,5′,6,6′-tetrachloro-1,1′, 3,3′-tetraethylbenzimidazol-carbocyanine iodide). After 30 min of incubation in a 5% CO_2 incubator, and after two washing steps with HBSS, fluorescence intensity (Ex/Em 485/535 nm) was measured in using the Ascent fluorescence reader (Thermo Fisher Scientific). Fluorescence values (RFU) were finally expressed as % of controls with n = 3 (each done in duplicates).

4.8 Determination of mRNA expression of BDNF by RT-qPCR

mRNA was isolated directly from SH-SY5Y$_{ATRA}$ derived from the incubation experiments using the Dynabeads mRNA DIRECT™ kit (Invitrogen GmbH) according to the manufacturer's instructions. After the isolation of mRNA, cDNA synthesis was carried out with the iScript cDNA synthesis kit using the C1000 Touch Thermal cycler (Bio-Rad Laboratories GmbH, Feldkirchen, Germany) in a reaction volume of 10 µL containing 20 ng mRNA with iScript reaction mix (5×), iScript Reverse Transcriptase and nuclease-free water (Bio-Rad Laboratories GmbH). Samples were incubated at 25°C for 5 min, followed by an incubation at 46°C for 20 min, and inactivation at 95°C for 1 min. Amplification of target genes (BDNF and ß-Actin (ACTB)) was measured using the C1000 Touch Thermal cycler (Bio-Rad Laboratories GmbH, Feldkirchen, Germany) with gene-specific primers/probe sets labeled with FAM (BDNF-PrimePCR™ Probe Assay) or HEX (ACTB-PrimePCR™ Probe Assay). Amplification were done with 2 µL cDNA in a reaction volume of 20 µL containing iTaq Universal Probes Supermix (2×), PrimePCR™ Probe Assay (Bio-Rad Laboratories GmbH), and water in a two-step amplification with 3 min of initial denaturation at 95°C, followed by 45 cycles of 5 s at 95°C and 30 s at 60°C. The relative expression level was measured using the ΔΔ C_T-method, in which ΔC_T was calculated by subtracting the C_T value of ACTB from the specific C_T value of the BDNF. ΔΔ C_T was obtained by subtracting the Δ C_T of each experimental sample by the Δ C_T of a positive control (92, 93). Expression levels were given as % of control with $n = 3$ (each done in duplicates).

4.9 Inhibition of BDNF-secretion by calcium channel blocker verapamil

Inhibition of BNDF secretion was measured using BDNF Quantikine™ ELISA Kit (R&D GmbH, Heidelberg, Germany) as described above (see Section 4.4). Briefly, before incubation of SH-SY5YATRA cells with supernatants from batch culture collection at stat-growth phase, cells were washed twice with pre-warmed HBSS and were then pre-incubated for 30 min with 7.5 µM or without verapamil (> 99%; Calbiochem®, Merck, Germany). Afterward, the cells were washed twice with medium and finally incubated with the metabolite enriched media. Briefly, after 24 h of incubation, supernatants were collected and stored at −20°C until analysis for BDNF. Data are given as pg./mL with n = 3 (each in duplicate).

4.10 Flow cytometry analysis for TrkB expression

For cytometry analysis, cells were treated with accutase solution (Promocell, Heidelberg, Germany) for 10 min to ensure surface protein integrity. For TrkA staining cells were centrifugated (500 × *g*, 10 min) and stained immediately with anti-human TrkA PE-conjugated REAfinity antibody (Miltenyi Biotec B.V. & Co. KG) for 10 min in the dark (Table 2). For TrkB staining, cells were incubated after centrifugation with F_C-blocking reagent (Miltenyi Biotec B.V. & Co. KG) for 15 min. Then, cells were incubated with mouse anti-human TrkB Alexa Fluor® 405-conjugated monoclonal antibody or Alexa Fluor® 405-conjugated isotype control (IgG_1) antibody (R&D GmbH) for 10 min in the dark at room temperature. Unbound antibodies were removed by washing the cells in 1 mL running buffer (Miltenyi Biotec B.V. & Co. KG) and after centrifugation (500 × *g*, 10 min), cells were resuspended in 200 µL of running buffer for final flow cytometry analysis. Cell gating strategy and quantification (see Figure 6) were performed using the MACSQuant 2.13.0 software (Miltenyi Biotec B.V. & Co. KG) by comparing the median fluorescence intensities (MFI) of unstained, isotype stained, and Trk-stained cells with n = 3 (each done in duplicates).

4.11 Statistical analysis

Statistical analyses were carried out using GraphPad Prism 10.0.2 (GraphPad Software, MA, United States) As indicated, data were

TABLE 2 Antibodies for Trk staining of SH-SY5Y and SH-SY5Y$_{ATRA}$ cell.

Target	Primary recombinant antibodies (Ab)	Fluorochrome	Dilution	Incubation time	MQ10 channel
TrkA	REAfinity®	PE	1:50	10 min	B2 (PE)
TrkB	Monoclonal anti-human	Alexa Flour® 405	1:50	10 min	V1 (Vioblue)
Isotype control	Monoclonal mouse IgG1	Alexa Flour® 405	1:50	10 min	V1 (Vioblue)

analyzed by one-way ANOVA and multicomparison test or *t*-test. Differences were considered significant at $^{*}p < 0.05$, $^{**}p < 0.01$, and $^{***}p < 0.001$.

Data availability statement

The original contributions presented in the study are included in the article/Supplementary material, further inquiries can be directed to the corresponding author.

Ethics statement

Ethical approval was not required for the studies on humans in accordance with the local legislation and institutional requirements because only commercially available established cell lines were used.

Author contributions

SK: Conceptualization, Data curation, Formal analysis, Investigation, Methodology, Validation, Visualization, Writing – original draft, Writing – review & editing. CK: Conceptualization, Funding acquisition, Resources, Writing – review & editing. CB: Investigation, Writing – review & editing. DH: Writing – review & editing. SM: Writing – review & editing. RB: Conceptualization, Writing – review & editing. SR: Conceptualization, Funding acquisition, Methodology, Project administration, Resources, Supervision, Validation, Writing – original draft, Writing – review & editing.

Funding

The author(s) declare financial support was received for the research, authorship, and/or publication of this article. The study received funding from Abbott Nutrition as institutional funding. The funder was involved in the conceptualization of the study, but not in the collection, analysis, and interpretation of data or the decision to submit the article for publication.

Acknowledgments

The authors are grateful to Katrin Koslowski and Cordula Becker for their excellent technical assistance and to Sylvia Schnell and Stefan Ratering for their supporting help with microbial cultivation.

Conflict of interest

DH, SM, and RB were employed by Abbott, Nutrition Division.

The remaining authors declare that the research was conducted in the absence of any commercial or financial relationships that could be construed as a potential conflict of interest.

Publisher's note

Supplementary material

The Supplementary material for this article can be found online at: https://www.frontiersin.org/articles/10.3389/fnut.2024.1351433/full#supplementary-material

References

1. Austin S, de Castro C, Bénet T, Hou Y, Sun H, Thakkar SK, et al. Temporal change of the content of 10 oligosaccharides in the Milk of Chinese urban mothers. *Nutrients*. (2016) 8:346. doi: 10.3390/nu8060346

2. Urashima T, Hirabayashi J, Sato S, Kobata A. Human Milk oligosaccharides as essential tools for basic and application studies on galectins. *Trends Glycosci Glycotechnol*. (2018) 30:SE51–65. doi: 10.4052/tigg.1734.1SE

3. Kunz C, Meyer C, Collado MC, Geiger L, García-Mantrana I, Bertua-Ríos B, et al. Influence of gestational age, secretor, and Lewis blood group status on the oligosaccharide content of human Milk. *J Pediatr Gastroenterol Nutr*. (2017) 64:789–98. doi: 10.1097/MPG.0000000000001402

4. Bode L. Human milk oligosaccharides. Every baby needs a sugar mama. *Glycobiology*. (2012) 22:1147–62. doi: 10.1093/glycob/cws074

5. Thurl S, Munzert M, Boehm G, Matthews C, Stahl B. Systematic review of the concentrations of oligosaccharides in human milk. *Nutr Rev*. (2017) 75:920–33. doi: 10.1093/nutrit/nux044

6. Erney RM, Malone WT, Skelding MB, Marcon AA, Kleman–Leyer KM, O'Ryan ML, et al. Variability of human milk neutral oligosaccharides in a diverse population. *J Pediatr Gastroenterol Nutr*. (2000) 30:181–92. doi: 10.1097/00005176-200002000-00016

7. Coppa GV, Gabrielli O, Zampini L, Galeazzi T, Ficcadenti A, Padella L, et al. Oligosaccharides in 4 different milk groups, Bifidobacteria, and *Ruminococcus obeum*. *J Pediatr Gastroenterol Nutr*. (2011) 53:80–7. doi: 10.1097/MPG.0b013e3182073103

8. McGuire MK, Meehan CL, McGuire MA, Williams JE, Foster J, Sellen DW, et al. What's normal? Oligosaccharide concentrations and profiles in milk produced by

healthy women vary geographically. *Am J Clin Nutr*. (2017) 105:1086–00. doi: 10.3945/ajcn.116.139980

9. Ruiz-Moyano S, Totten SM, Garrido DA, Smilowitz JT, German JB, Lebrilla CB, et al. Variation in consumption of human milk oligosaccharides by infant gut-associated strains of *Bifidobacterium breve*. *Appl Environ Microbiol*. (2013) 79:6040–9. doi: 10.1128/AEM.01843-13

10. Yu Z-T, Chen C, Kling DE, Liu B, McCoy JM, Merighi M, et al. The principal fucosylated oligosaccharides of human milk exhibit prebiotic properties on cultured infant microbiota. *Glycobiology*. (2013) 23:169–77. doi: 10.1093/glycob/cws138

11. Cilieborg MS, Sangild PT, Jensen ML, Østergaard MV, Christensen L, Rasmussen SO, et al. α1,2-Fucosyllactose does not improve intestinal function or prevent *Escherichia coli* F18 diarrhea in newborn pigs. *J Pediatr Gastroenterol Nutr*. (2017) 64:310–8. doi: 10.1097/MPG.0000000000001276

12. Schack-Nielsen L, Michaelsen KF. Advances in our understanding of the biology of human milk and its effects on the offspring. *J Nutr*. (2007) 137:503S–10S. doi: 10.1093/jn/137.2.503S

13. Kramer MS, Aboud F, Mironova E, Vanilovich I, Platt RW, Matush L, et al. Breastfeeding and child cognitive development. New evidence from a large randomized trial. *Arch Gen Psychiatry*. (2008) 65:578–84. doi: 10.1001/archpsyc.65.5.578

14. Horta BL, De Mola CL, Victora CG. Breastfeeding and intelligence: a systematic review and meta-analysis. *Acta Paediatr*. (2015) 104:14–9. doi: 10.1111/apa.13139

15. Horta BL, De Sousa BA, De Mola CL. Breastfeeding and neurodevelopmental outcomes. *Curr Opin Clin Nutr Metabol Care*. (2018) 21:174–8. doi: 10.1097/MCO.0000000000000453

16. Liu F, Simpson AB, D'Costa E, Bunn FS, van Leeuwen SS. Sialic acid, the secret gift for the brain. *Crit Rev Food Sci Nutr*. (2023) 63:9875–94. doi: 10.1080/10408398.2022.2072270

17. Vázquez E, Barranco A, Ramírez M, Gruart A, Delgado-García JM, Martínez-Lara E, et al. Effects of a human milk oligosaccharide, 2′-fucosyllactose, on hippocampal long-term potentiation and learning capabilities in rodents. *J Nutr Biochem*. (2015) 26:455–65. doi: 10.1016/j.jnutbio.2014.11.016

18. Berger PK, Plows JF, Jones RB, Alderete TL, Yonemitsu C, Poulsen M, et al. Human milk oligosaccharide 2′-fucosyllactose links feedings at 1 month to cognitive development at 24 months in infants of normal and overweight mothers. *PLoS One*. (2020) 15:e0228323. doi: 10.1371/journal.pone.0228323

19. Wu K-J, Chen Y-H, Bae E-K, Song Y, Min W, Yu S-J. Human Milk oligosaccharide 2'-Fucosyllactose reduces neurodegeneration in stroke brain. *Transl Stroke Res*. (2020) 11:1001–11. doi: 10.1007/s12975-019-00774-z

20. Oliveros E, Ramirez M, Vazquez E, Barranco A, Gruart A, Delgado-Garcia JM, et al. Oral supplementation of 2′-fucosyllactose during lactation improves memory and learning in rats. *J Nutr Biochem*. (2016) 31:20–7. doi: 10.1016/j.jnutbio.2015.12.014

21. Berger PK, Bansal R, Sawardekar S, Yonemitsu C, Furst A, Hampson HE, et al. Associations of human Milk oligosaccharides with infant brain tissue organization and regional blood flow at 1 month of age. *Nutrients*. (2022) 14:3820. doi: 10.3390/nu14183820

22. Anders QS, Ferreira LVB, Rodrigues LCM, Nakamura-Palacios EM. BDNF mRNA expression in leukocytes and frontal cortex function in drug use disorder. *Front Psych*. (2020) 11:469. doi: 10.3389/fpsyt.2020.00469

23. Waterhouse EG, An JJ, Orefice LL, Baydyuk M, Liao GY, Zheng K, et al. BDNF promotes differentiation and maturation of adult-born neurons through GABAergic transmission. *J Neurosci*. (2012) 32:14318–30. doi: 10.1523/JNEUROSCI.0709-12.2012

24. Leal G, Comprido D, Duarte CB. BDNF-induced local protein synthesis and synaptic plasticity. *Neuropharmacology*. (2014) 76:639–56. doi: 10.1016/j.neuropharm.2013.04.005

25. Cunha C, Brambilla R, Thomas KL. A simple role for BDNF in learning and memory? *Front Mol Neurosci*. (2010) 3:1. doi: 10.3389/neuro.02.001.2010

26. Colucci-D'Amato L, Speranza L, Volpicelli F. Neurotrophic factor BDNF, physiological functions and therapeutic potential in depression, neurodegeneration and brain Cancer. *Int J Mol Sci*. (2020) 21:7777. doi: 10.3390/ijms21207777

27. Gottmann K, Mittmann T, Lessmann V. BDNF signaling in the formation, maturation and plasticity of glutamatergic and GABAergic synapses. *Exp Brain Res*. (2009) 199:203–34. doi: 10.1007/s00221-009-1994-z

28. Kuntz S, Kunz C, Borsch C, Vazquez E, Buck R, Reutzel M, et al. Metabolic fate and distribution of 2′-Fucosyllactose: direct influence on gut microbial activity but not on brain. *Mol Nutr Food Res*. (2019) 63:e1900035. doi: 10.1002/mnfr.201900035

29. Rudloff S, Kuntz S, Borsch C, Vazquez E, Buck R, Reutzel M, et al. Fucose as a cleavage product of 2'Fucosyllactose does not cross the blood-brain barrier in mice. *Mol Nutr Food Res*. (2021) 65:e2100045. doi: 10.1002/mnfr.202100045

30. Salli K, Hirvonen J, Siitonen J, Ahonen I, Anglenius H, Maukonen J. Selective utilization of the human Milk oligosaccharides 2'-Fucosyllactose, 3-Fucosyllactose, and Difucosyllactose by various probiotic and pathogenic Bacteria. *J Agric Food Chem*. (2021) 69:170–82. doi: 10.1021/acs.jafc.0c06041

31. Nogacka AM, Arboleya S, Nikpoor N, Auger J, Salazar N, Cuesta I, et al. Influence of 2'-Fucosyllactose on the microbiota composition and metabolic activity of fecal cultures from breastfed and formula-fed infants at two months of age. *Microorganisms*. (2021) 9:1478. doi: 10.3390/microorganisms9071478

32. Underwood MA, Gaerlan S, De Leoz MLA, Dimapasoc L, Kalanetra KM, Lemay DG, et al. Human milk oligosaccharides in premature infants: absorption, excretion, and influence on the intestinal microbiota. *Pediatr Res*. (2015) 78:670–7. doi: 10.1038/pr.2015.162

33. Rudloff S, Pohlentz G, Borsch C, Lentze MJ, Kunz C. Urinary excretion of in vivo ^{13}C-labelled milk oligosaccharides in breastfed infants. *Br J Nutr*. (2012) 107:957–63. doi: 10.1017/S0007114511004016

34. Dotz V, Rudloff S, Blank D, Lochnit G, Geyer R, Kunz C. 13C-labeled oligosaccharides in breastfed infants' urine: individual-, structure- and time-dependent differences in the excretion. *Glycobiology*. (2014) 24:185–94. doi: 10.1093/glycob/cwt099

35. Dotz V, Rudloff S, Meyer C, Lochnit G, Kunz C. Metabolic fate of neutral human milk oligosaccharides in exclusively breast-fed infants. *Mol Nutr Food Res*. (2015) 59:355–64. doi: 10.1002/mnfr.201400160

36. Dotz V, Adam R, Lochnit G, Schroten H, Kunz C. Neutral oligosaccharides in feces of breastfed and formula-fed infants at different ages. *Glycobiology*. (2016) 26:1308–16. doi: 10.1093/glycob/cww087

37. Goehring KC, Kennedy AD, Prieto PA, Buck RH. Direct evidence for the presence of human milk oligosaccharides in the circulation of breastfed infants. *PLoS One*. (2014) 9:e101692. doi: 10.1371/journal.pone.0101692

38. Hill DR, Buck RH. Infants fed breastmilk or 2'-FL supplemented formula have similar systemic levels of microbiota-derived secondary bile acids. *Nutrients*. (2023) 15:2339. doi: 10.3390/nu15102339

39. Garrido D, Ruiz-Moyano S, Kirmiz N, Davis JC, Totten SM, Lemay DG, et al. A novel gene cluster allows preferential utilization of fucosylated milk oligosaccharides in *Bifidobacterium longum* subsp. longum SC596. *Sci Rep*. (2016) 6:35045. doi: 10.1038/srep35045

40. Ward RE, Niñonuevo M, Mills DA, Lebrilla CB, German JB. In vitro fermentability of human milk oligosaccharides by several strains of bifidobacteria. *Mol Nutr Food Res*. (2007) 51:1398–05. doi: 10.1002/mnfr.200700150

41. Yamada C, Gotoh A, Sakanaka M, Hattie M, Stubbs KA, Katayama-Ikegami A, et al. Molecular insight into evolution of Symbiosis between breast-fed infants and a member of the human gut microbiome *Bifidobacterium longum*. *Cell Chem Biol*. (2017) 24:515–524.e5. doi: 10.1016/j.chembiol.2017.03.012

42. Katayama T. Host-derived glycans serve as selected nutrients for the gut microbe. Human milk oligosaccharides and bifidobacteria. *Biosci Biotechol Biochemist*. (2016) 80:621–32. doi: 10.1080/09168451.2015.1132153

43. Milani C, Duranti S, Bottacini F, Casey E, Turroni F, Mahony J, et al. The first microbial colonizers of the human gut. Composition, activities, and health implications of the infant gut microbiota. Microbiology and molecular biology reviews. *Microbiol Mol Biol Rev*. (2017) 81:e00036-17. doi: 10.1128/MMBR.00036-17

44. Matsuki T, Yahagi K, Mori H, Matsumoto H, Hara T, Tajima S, et al. A key genetic factor for fucosyllactose utilization affects infant gut microbiota development. *Nat Commun*. (2016) 7:11939. doi: 10.1038/ncomms11939

45. Centanni M, Ferguson SA, Sims IM, Biswas A, Tannock GW. *Bifidobacterium bifidum* ATCC 15696 and *Bifidobacterium breve* 24b metabolic interaction based on 2'-O-Fucosyl-lactose studied in steady-state cultures in a Freter-style Chemostat. *Appl Environ Microbiol*. (2019) 85:e02783–18. doi: 10.1128/AEM.02783-18

46. Sakanaka M, Hansen ME, Gotoh A, Katoh T, Yoshida K, Odamaki T, et al. Evolutionary adaptation in fucosyllactose uptake systems supports bifidobacteria-infant symbiosis. *Sci Adv*. (2019) 5:eaaw7696. doi: 10.1126/sciadv.aaw7696

47. Zabel B, Yde CC, Roos P, Marcussen J, Jensen HM, Salli K, et al. Novel genes and metabolite trends in *Bifidobacterium longum* subsp. infantis bi-26 metabolism of human Milk oligosaccharide 2′-fucosyllactose. *Sci Rep*. (2019) 9:7983. doi: 10.1038/s41598-019-43780-9

48. Egan M, Motherway MO, Kilcoyne M, Kane M, Joshi L, Ventura M, et al. Cross-feeding by *Bifidobacterium breve* UCC2003 during co-cultivation with *Bifidobacterium bifidum* PRL2010 in a mucin-based medium. *BMC Microbiol*. (2014) 14:282. doi: 10.1186/s12866-014-0282-7

49. Turroni F, Bottacini F, Foroni E, Mulder I, Kim J-H, Zomer A, et al. Genome analysis of *Bifidobacterium bifidum* PRL2010 reveals metabolic pathways for host-derived glycan foraging. *Proc Natl Acad Sci USA*. (2010) 107:19514–9. doi: 10.1073/pnas.1011100107

50. Thongaram T, Hoeflinger JL, Chow J, Miller MJ. Human milk oligosaccharide consumption by probiotic and human-associated bifidobacteria and lactobacilli. *J Dairy Sci*. (2017) 100:7825–33. doi: 10.3168/jds.2017-12753

51. Cheung Y-T, Lau WK-W, Yu M-S, Lai CS-W, Yeung S-C, So K-F, et al. Effects of all-trans-retinoic acid on human SH-SY5Y neuroblastoma as in vitro model in neurotoxicity research. *Neurotoxicology*. (2009) 30:127–35. doi: 10.1016/j.neuro.2008.11.001

52. Cassiman D, van Pelt J, De Vos R, van Lommel F, Desmet V, Yap SH, et al. Synaptophysin: a novel marker for human and rat hepatic stellate cells. *Am J Pathol*. (1999) 155:1831–9. doi: 10.1016/S0002-9440(10)65501-0

53. Lepack AE, Fuchikami M, Dwyer JM, Banasr M, Duman RS. BDNF release is required for the behavioral actions of ketamine. *Int J Neuropsychopharmacol*. (2014) 18:pyu033. doi: 10.1093/ijnp/pyu033

54. Gonulalan E-M, Bayazeid O, Yalcin F-N, Demirezer L-O. The roles of valerenic acid on BDNF expression in the SH-SY5Y cell. *Saudi Pharm J*. (2018) 26:960–4. doi: 10.1016/j.jsps.2018.05.005

55. Numakawa T, Suzuki S, Kumamaru E, Adachi N, Richards M, Kunugi H. BDNF function and intracellular signaling in neurons. *Histol Histopathol*. (2010) 25:237–58. doi: 10.14670/HH-25.237

56. Colombo E, Cordiglieri C, Melli G, Newcombe J, Krumbholz M, Parada LF, et al. Stimulation of the neurotrophin receptor TrkB on astrocytes drives nitric oxide production and neurodegeneration. *J Exp Med*. (2012) 209:521–35. doi: 10.1084/jem.20110698

57. Nassenstein C, Möhring UH, Luttmann W, Virchow JC, Braun A. Differential expression of the neurotrophin receptors p75NTR, TrkA, TrkB and TrkC in human peripheral blood mononuclear cells. *Exp Toxicol Pathol*. (2006) 57:55–63. doi: 10.1016/j.etp.2006.02.008

58. Islam O, Loo TX, Heese K. Brain-derived neurotrophic factor (BDNF) has proliferative effects on neural stem cells through the truncated TRK-B receptor, MAP kinase, AKT, and STAT-3 signaling pathways. *Curr Neurovasc Res*. (2009) 6:42–53. doi: 10.2174/156720209787466028

59. De Medeiros LM, De Bastiani MA, Rico EP, Schonhofen P, Pfaffenseller B, Wollenhaupt-Aguiar B, et al. Cholinergic differentiation of human neuroblastoma SH-SY5Y cell line and its potential use as an in vitro model for Alzheimer's disease studies. *Mol Neurobiol*. (2019) 56:7355–67. doi: 10.1007/s12035-019-1605-3

60. Chiu Y-J, Lin T-H, Chang K-H, Lin W, Hsieh-Li HM, Su M-T, et al. Novel TRKB agonists activate TRKB and downstream ERK and AKT signaling to protect Aβ-GFP SH-SY5Y cells against Aβ toxicity. *Aging*. (2022) 14:7568–86. doi: 10.18632/aging.204306

61. Presgraves SP, Ahmed T, Borwege S, Joyce JN. Terminally differentiated SH-SY5Y cells provide a model system for studying neuroprotective effects of dopamine agonists. *Neurotox Res*. (2004) 5:579–98. doi: 10.1007/BF03033178

62. Martin E-R, Gandawijaya J, Oguro-Ando A. A novel method for generating glutamatergic SH-SY5Y neuron-like cells utilizing B-27 supplement. *Front Pharmacol*. (2022) 13:943627. doi: 10.3389/fphar.2022.943627

63. Kovalevich J, Langford D. Considerations for the use of SH-SY5Y neuroblastoma cells in neurobiology. *Methods Mol Biol*. (2013) 1078:9–21. doi: 10.1007/978-1-62703-640-5_2

64. Fleming SA, Mudd AT, Hauser J, Yan J, Metairon S, Steiner P, et al. Human and bovine Milk oligosaccharides elicit improved recognition memory concurrent with alterations in regional brain volumes and hippocampal mRNA expression. *Front Neurosci*. (2020) 14:770. doi: 10.3389/fnins.2020.00770

65. Hauser J, Pisa E, Arias Vásquez A, Tomasi F, Traversa A, Chiodi V, et al. Sialylated human milk oligosaccharides program cognitive development through a non-genomic transmission mode. *Mol Psychiatry*. (2021) 26:2854–71. doi: 10.1038/s41380-021-01054-9

66. Mortensen EL, Michaelsen KF, Sanders SA, Reinisch JM. The association between duration of breastfeeding and adult intelligence. *JAMA*. (2002) 287:2365–71. doi: 10.1001/jama.287.18.2365

67. Wang J, Cheng A, Wakade C, Yu RK. Ganglioside GD3 is required for neurogenesis and long-term maintenance of neural stem cells in the postnatal mouse brain. *J Neurosci*. (2014) 34:13790–800. doi: 10.1523/JNEUROSCI.2275-14.2014

68. Matthies H, Staak S, Krug M. Fucose and fucosyllactose enhance in-vitro hippocampal long-term potentiation. *Brain Res*. (1996) 725:276–80. doi: 10.1016/0006-8993(96)00406-4

69. Krug M, Wagner M, Staak S, Smalla KH. Fucose and fucose-containing sugar epitopes enhance hippocampal long-term potentiation in the freely moving rat. *Brain Res*. (1994) 643:130–5. doi: 10.1016/0006-8993(94)90018-3

70. Murrey HE, Hsieh-Wilson LC. The chemical neurobiology of carbohydrates. *Chem Rev*. (2008) 108:1708–31. doi: 10.1021/cr078215f

71. Lee S, Goodson ML, Vang W, Rutkowsky J, Kalanetra K, Bhattacharya M, et al. Human milk oligosaccharide 2′-fucosyllactose supplementation improves gut barrier function and signaling in the vagal afferent pathway in mice. *Food Funct*. (2021) 12:8507–21. doi: 10.1039/d1fo00658d

72. Li H, Lane JA, Chen J, Lu Z, Wang H, Dhital S, et al. In vitro fermentation of human milk oligosaccharides by individual *Bifidobacterium longum*-dominant infant fecal inocula. *Carbohydr Polym*. (2022) 287:119322. doi: 10.1016/j.carbpol.2022.119322

73. Wang J, Chen M-S, Wang R-S, Hu J-Q, Liu S, Wang Y-Y, et al. Current advances in structure-function relationships and dose-dependent effects of human Milk oligosaccharides. *J Agric Food Chem*. (2022) 70:6328–53. doi: 10.1021/acs.jafc.2c01365

74. Lawson MAE, O'Neill IJ, Kujawska M, Gowrinadh Javvadi S, Wijeyesekera A, Flegg Z, et al. Breast milk-derived human milk oligosaccharides promote Bifidobacterium interactions within a single ecosystem. *ISME J*. (2020) 14:635–48. doi: 10.1038/s41396-019-0553-2

75. Asakuma S, Hatakeyama E, Urashima T, Yoshida E, Katayama T, Yamamoto K, et al. Physiology of consumption of human milk oligosaccharides by infant gut-associated bifidobacteria. *J Biol Chem*. (2011) 286:34583–92. doi: 10.1074/jbc.M111.248138

76. Dedon LR, Özcan E, Rani A, Sela DA. *Bifidobacterium infantis* metabolizes 2'Fucosyllactose-derived and free Fucose through a common catabolic pathway resulting in 1,2-Propanediol secretion. *Front Nutr*. (2020) 7:583397. doi: 10.3389/fnut.2020.583397

77. Le HTQ, Lee EY. Insights into C1 and C3 assimilation pathways in type I methanotrophic bacterium from co-production of 1,2-propanediol and lactate. *Bioresour Technol*. (2022) 365:128172. doi: 10.1016/j.biortech.2022.128172

78. Bunesova V, Lacroix C, Schwab C. Fucosyllactose and L-fucose utilization of infant Bifidobacterium longum and *Bifidobacterium kashiwanohense*. *BMC Microbiol*. (2016) 16:248. doi: 10.1186/s12866-016-0867-4

79. Newman LA, Korol DL, Gold PE. Lactate produced by glycogenolysis in astrocytes regulates memory processing. *PLoS One*. (2011) 6:e28427. doi: 10.1371/journal.pone.0028427

80. Müller P, Duderstadt Y, Lessmann V, Müller NG. Lactate and BDNF: key mediators of exercise induced neuroplasticity? *J Clin Med*. (2020) 9:1136. doi: 10.3390/jcm9041136

81. El Hayek L, Khalifeh M, Zibara V, Abi Assaad R, Emmanuel N, Karnib N, et al. Lactate mediates the effects of exercise on learning and memory through SIRT1-dependent activation of hippocampal brain-derived neurotrophic factor (BDNF). *J Neurosci*. (2019) 39:2369–82. doi: 10.1523/JNEUROSCI.1661-18.2019

82. Lee WJ, Lee GH, Hur J, Lee HG, Kim E, Won JP, et al. Taurine and Ginsenoside Rf induce BDNF expression in SH-SY5Y cells: a potential role of BDNF in corticosterone-triggered cellular damage. *Molecules*. (2020) 25:2819. doi: 10.3390/molecules25122819

83. Brewis IA, Morton IE, Mohammad SN, Browes CE, Moore HD. Measurement of intracellular calcium concentration and plasma membrane potential in human spermatozoa using flow cytometry. *J Androl*. (2000) 21:238–49. doi: 10.1002/j.1939-4640.2000.tb02101.x

84. Kato T, Fogaça MV, Deyama S, Li X-Y, Fukumoto K, Duman RS. BDNF release and signaling are required for the antidepressant actions of GLYX-13. *Mol Psychiatry*. (2018) 23:2007–17. doi: 10.1038/mp.2017.220

85. Fukumoto K, Fogaça MV, Liu R-J, Duman C, Kato T, Li X-Y, et al. Activity-dependent brain-derived neurotrophic factor signaling is required for the antidepressant actions of (2R,6R)-hydroxynorketamine. *Proc Natl Acad Sci USA*. (2019) 116:297–02. doi: 10.1073/pnas.1814709116

86. Encinas M, Iglesias M, Llecha N, Comella JX. Extracellular-regulated kinases and phosphatidylinositol 3-kinase are involved in brain-derived neurotrophic factor-mediated survival and neuritogenesis of the neuroblastoma cell line SH-SY5Y. *J Neurochem*. (1999) 73:1409–21. doi: 10.1046/j.1471-4159.1999.0731409.x

87. Encinas M, Iglesias M, Liu Y, Wang H, Muhaisen A, Ceña V, et al. Sequential treatment of SH-SY5Y cells with retinoic acid and brain-derived neurotrophic factor gives rise to fully differentiated, neurotrophic factor-dependent, human neuron-like cells. *J Neurochem*. (2000) 75:991–03. doi: 10.1046/j.1471-4159.2000.0750991.x

88. Kuntz S, Asseburg H, Dold S, Römpp A, Fröhling B, Kunz C, et al. Inhibition of low-grade inflammation by anthocyanins from grape extract in an in vitro epithelial-endothelial co-culture model. *Food Funct*. (2015) 6:1136–49. doi: 10.1039/c4fo00755g

89. Teppola H, Sarkanen J-RJalonen TO, Linne M-L. Morphological differentiation towards neuronal phenotype of SH-SY5Y neuroblastoma cells by estradiol. *Retinoic Acid Cholesterol Neurochem Res*. (2016) 41:731–47. doi: 10.1007/s11064-015-1743-6

90. Al-Maswary AA, O'Reilly M, Holmes AP, Walmsley AD, Cooper PR, Scheven BA. Exploring the neurogenic differentiation of human dental pulp stem cells. *PLoS One*. (2022) 17:e0277134. doi: 10.1371/journal.pone.0277134

91. Sakamuru S, Attene-Ramos MS, Xia M. Mitochondrial membrane potential assay. *Methods Mol Biol*. (2016) 1473:17–22. doi: 10.1007/978-1-4939-6346-1_2

92. Kuntz S, Rudloff S, Kunz C. Oligosaccharides from human milk influence growth-related characteristics of intestinally transformed and non-transformed intestinal cells. *Br J Nutr*. (2008) 99:462–71. doi: 10.1017/S0007114507824068

93. Kuntz S, Kunz C, Rudloff S. Inhibition of pancreatic cancer cell migration by plasma anthocyanins isolated from healthy volunteers receiving an anthocyanin-rich berry juice. *Eur J Nutr*. (2017) 56:203–14. doi: 10.1007/s00394-015-1070-3